Global and Planetary Change 74 (2010) 99–113

Contents lists available at ScienceDirect

Global and Planetary Change

journal homepage: www.elsevier.com/locate/gloplacha

Records of environmental changes during the Holocene from Isla de los Estados (54.4°S), southeastern Tierra del Fuego

Ingmar Unkel [a,b,*], Marilen Fernandez [a,c], Svante Björck [a], Karl Ljung [a,d], Barbara Wohlfarth [e]

[a] Department of Earth and Ecosystem Sciences, Division of Geology, Quaternary Sciences, Lund University, Sölvegatan 12, SE-223 62 Lund, Sweden
[b] Graduate School "Human Development in Landscapes", c/o Institute for Ecosystem Research, Kiel University, Olshausenstr. 75, DE-24118 Kiel, Germany
[c] Quaternary Laboratory, CADIC-CONICET, 9410 Ushuaia, Tierra del Fuego, Argentina
[d] Organic Geochemistry Unit, Biogeochemistry Research Centre, School of Chemistry, Cantocks Close, University of Bristol, BS8 1TS, Bristol, United Kingdom
[e] Department of Geology and Geochemistry, Stockholm University, SE-10691 Stockholm, Sweden

ARTICLE INFO

Article history:
Received 17 December 2009
Accepted 1 July 2010
Available online 14 October 2010

Keywords:
Holocene
lake sediments
peat
diatom analysis
XRF
paleoclimate
southern westerlies
sea-level changes
Tierra del Fuego

ABSTRACT

Southernmost Patagonia, located at the relatively narrow passage between Antarctica and South America, is a highly sensitive region for recording meridional and zonal changes in the pattern of oceanic and atmospheric circulation. The island of Isla de los Estados, situated at 54.5°S, 64°W, east of Argentinean Tierra del Fuego, provides an exceptional possibility, to investigate terrestrial records of atmospheric conditions in an oceanic setting during the last deglaciation and the Holocene. Here we present geochemical and diatom analyses from 10 600 to c. 1500 cal BP of one sequence (LGB) with peat, lake sediments and lagoon deposits at the northern coast of the island, and a lake sediment sequence (CAS) 3 km further inland. The data comprise TC, TN, loss on ignition analyses and continuous XRF scanning as well as age–depth modeling based on AMS-^{14}C dating on both cores. Diatom analysis of the CAS record complements the geochemical proxies. During the Holocene, our two sites have been impacted by two different forcings: changes in the regional climate regime largely influenced by the varying strength and position of the Southern Hemisphere Westerlies (SHW), while relative sea-level changes affected the deposits of the coastal site. In concert with the onset of the Antarctic thermal optimum, our data suggest fairly warm conditions and the establishment of denser peat and forest vegetation on the island c. 10 600 cal BP. Between 8500 and 4500 cal BP geochemistry and diatoms from the CAS record indicate stronger Westerlies at this latitude, which means higher wind speed or higher storm frequency and more precipitation, resulting in more pronounced surface run-off. After 4500 cal BP, the geochemical proxies and large changes in diatom assemblages indicate a decrease in precipitation, weaker winds and possibly cooler conditions, probably as an effect of weaker SHW and/or a latitudinal shift. The depositional environment of CAS changed from gyttja to peat around 1000 cal BP. At LGB, the onset of gyttja sedimentation around 7900 cal BP shows that the former wet land with peat accumulation had become a lake with a fairly rapid sedimentation. The chemical data from LGB imply a gradually increasing marine influence, probably as an effect of both rising sea level and increased impact of storms and maximum high tides. After a marine high-stand during the mid-Holocene, the LGB site returned into a peat bog again around 3400 cal BP. Our data suggest that since then relative sea level first dropped back below present sea level followed by a rise to present day sea level.

1. Introduction

A dense network of sites, with well-dated proxy records, is necessary to comprehend the mechanisms behind the temporally and spatially highly variable Holocene climate (e.g. Mayewski et al., 2004). Regions with large climatic gradients, e.g. patterns in precipitation, temperature and wind speed/direction, are obvious key areas in this respect. Southernmost Tierra del Fuego is such an area, being situated between Antarctica and the main South American continent, separated by the Antarctic convergence (or Antarctic Polar Front). It is a region sensitive for meridional changes of the Westerlies and sea-ice extent, and is also a border area between the Pacific and Atlantic Southern Ocean. Holocene paleoclimatic records from Tierra del Fuego have therefore the potential to record such latitudinal shifts.

Here we present Holocene paleoenvironmental reconstructions based on lake sediments and peat deposits from the island of Isla de los Estados, east of Tierra del Fuego (Fig. 1).

* Corresponding author. Graduate School "Human Development in Landscapes", c/o Institute for Ecosystem Research, Kiel University, Olshausenstr. 75, DE-24118 Kiel, Germany. Tel.: +49 431 880 5241.
E-mail address: iunkel@ecology.uni-kiel.de (I. Unkel).

0921-8181/$ – see front matter © 2010 Elsevier B.V. All rights reserved.
doi:10.1016/j.gloplacha.2010.07.003

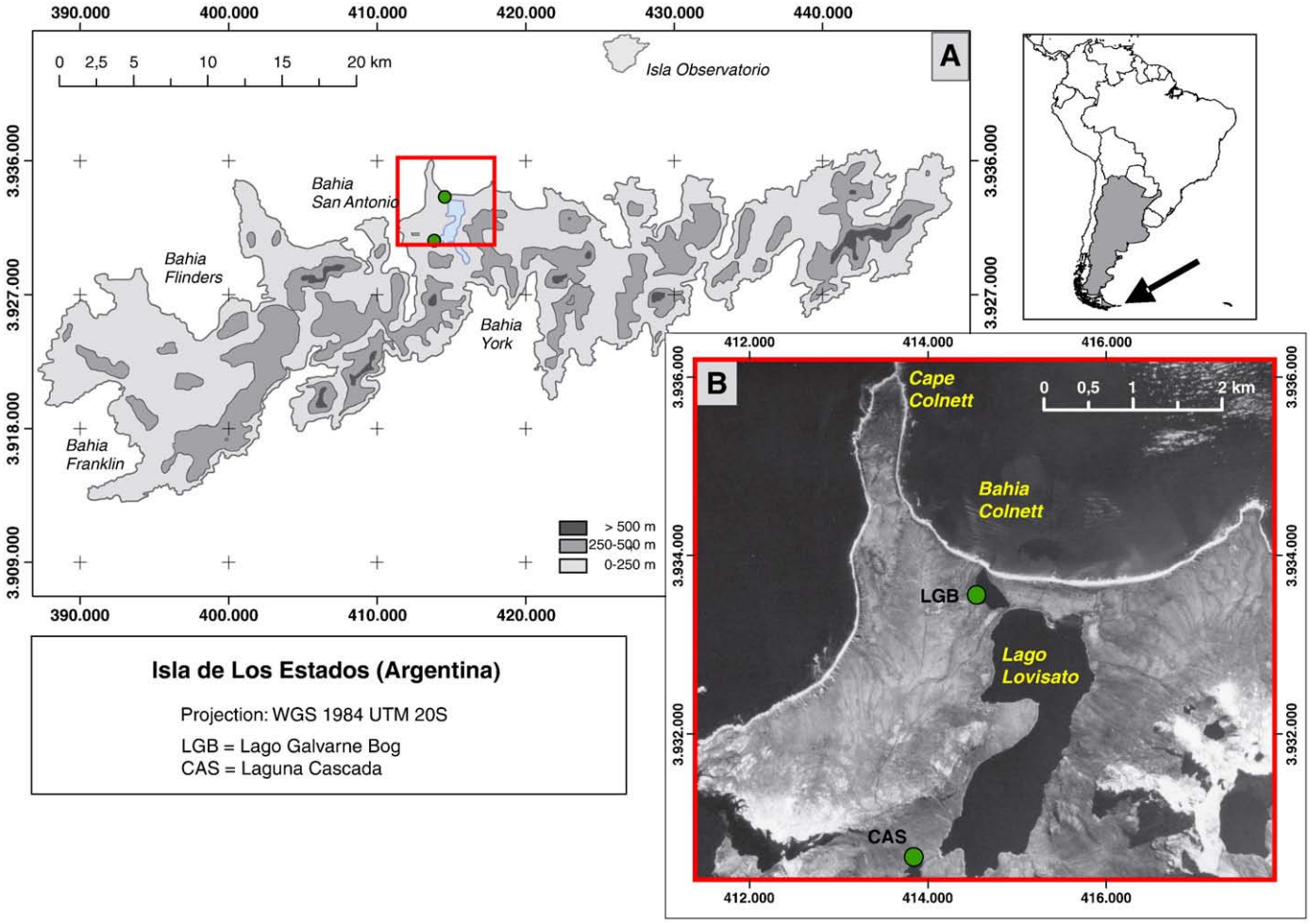

Fig. 1. (A) Map showing the position of the cored sites, Lago Galvarne Bog (LGB) and Laguna Cascada (CAS), on Isla de los Estados, and (B) magnification of the area marked with a square in (A).

2. Regional setting

The 65 km long, east–west elongated island of Isla de los Estados is situated about 40 km east of Isla Grande Tierra del Fuego at roughly 54° 45′S and between 64° 10′ and 63° 45′W (Fig. 1A,B). The island is between 1 and 14 km wide and its narrowest points occur where deeply incised fjords almost cut through, such as in Puerto Cook.

Climate is oceanic with a mean annual precipitation of around 1500 mm and January and July mean temperatures of 9.0 and 2.7 °C, respectively (Dudley and Crow, 1983). Strong winds, mainly from the southwest and west, prevail throughout the year. Maximum tidal range on the northern coast is c. 2.5 m.

Dudley and Crow (1983) recognized seven different vegetation types, which are mainly related to altitude and terrain forms. The oceanic conditions are best reflected by the typical *Nothofagus betuloides* and *Drimys winteri* evergreen forest with extremely dense, often almost impenetrable shrub and bryophyte undergrowth. Above approximately 450 m altitude the so-called Alpine Formation occurs with sparse vegetation cover, often including dwarfed forms of *Nothofagus antarctica* and *Empetrum rubrum* (Fig. 2A).

The island constitutes the eastern termination of the Andean Cordillera and its highest peaks reach up to 800 m a.s.l. Bedrock consists of Upper Jurassic to Lower Cretaceous volcanic rocks (Dalziel et al., 1974; Caminos and Nullo, 1979), which are dominated by thick acidic tuffs, lavas and ignimbrites, and which are occasionally overlain by black shales, calcareous mudstones, graywackes and limestones. Quaternary fluvial and aeolian sands occur inside Bahia Franklin and Holocene peat covers large parts of the lowlands. Sections with Quaternary diamicts and sorted deposits are found along the coast of some of the Northern capes and peninsulas as well as raised beach deposits in some of the bays.

Peat accumulation started in the coastal areas of Isla de los Estados around 16100 cal BP, indicating that the island must have been at least partially ice free at this time, while lake sediments from the inner part of the island suggest that the last mountain ice caps disappeared at the latest around 10600 cal BP (Unkel et al., 2008).

3. Materials and methods

Field work was performed in November–December 2005. From the base camp in Bahia Colnett (Fig. 2B), coring was carried out at the bog at Lago Galvarne, here called Lago Galvarne Bog and in Laguna Cascada (Fig. 2C), following detailed reconnaissance.

Lago Galvarne (c. 125000 m^2) is situated close to the northern sea shore and is separated from Lago Lovisato in the southeast by a distinct ice-marginal moraine (Möller et al., 2010). Laguna Cascada is a small lake (c. 13000 m^2) at the foothills of the mountain chain and glacial cirques are common on the steep mountain side south of the lake.

Coring was performed with a Russian chamber corer with diameters of 5 and 7.5 cm, respectively, and a chamber length of 1 m. Overlap between individual one-meter sections was at least 20 cm. A 745 cm thick sequence was recovered from Lago Galvarne Bog at the southern shore of the lake (54° 44′ 16.7″S, 64° 19′ 37.9″W; 2 m a.s.l.). At Laguna Cascada coring was performed on the quagmire

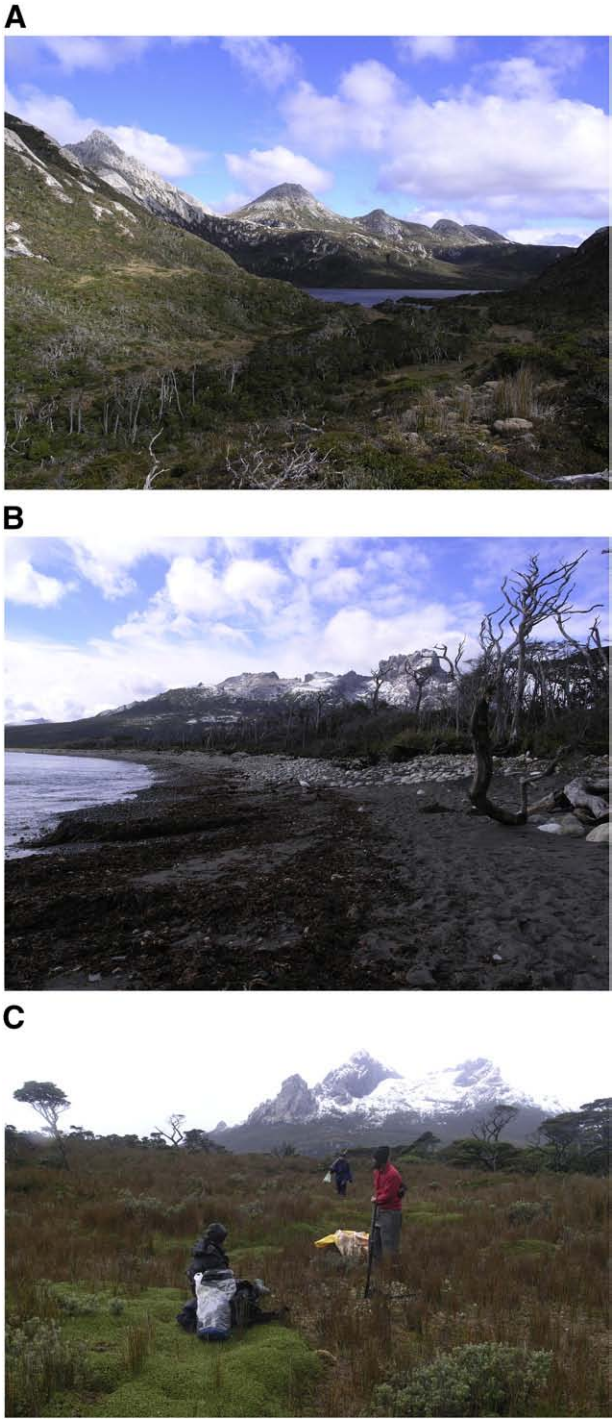

Fig. 2. (A) Alpine landscape on central Isla de los Estados. The vegetation on the lower parts of the slopes is dominated by *Nothofagus betuloides* forest. (B) View of the beach ridge damming Lago Galvarne. The photo is taken towards the east from close to the present day outlet of Lago Galvarne through the beach cobbles. The beach ridge is currently being eroded by the sea and trees on the beach ridge are dying because of the higher sea level. (C) Peat land close to the coring site of Laguna Cascada. Coring was done from peat extending out into the lake as a quagmire (photos taken by K. Ljung).

northeast of the lake (54° 45′ 51.3″S, 64° 20′ 20.7″W; ca. 10 m a.s.l.), where 523 cm of sediments were retrieved.

The sediment cores were described in the field, wrapped in plastic film, stored in PVC tubes and transported by ship to Sweden, where they were kept in a cold room until sub-sampling.

Magnetic susceptibility (κ) was measured using a Bartington MS2E1 high resolution surface scanning sensor coupled to a TAMISCAN automatic logging conveyor. The magnetic susceptibility gives a relative estimate of the magnetic mineral concentration in the sediments.

Loss on ignition (LOI) was measured to determine the amount of organic matter. Samples were dried at 105 °C for 12 h, weighed and combusted at 550 °C for 6 h.

Total carbon (TC) and total nitrogen (TN) concentrations were measured on a Costech Instruments ECS 4010 elemental analyzer. Samples were dried and homogenized before analysis. Standards (70% C and 10% N) were analyzed before, during and after analyses. The lack of carbonates in the sediments implies that TC is equivalent to total organic carbon (TOC). TC/TN ratios are used as a measure of terrestrial versus limnic organic matter (Meyers and Teranes, 2001) and we refer to the atomic ratio which is equivalent to 1.167 C/N mass ratio. Total sulphur (TS) was also measured on the Lago Galvarne Bog gyttja between 375 and 260 cm depth using the same instrument as for TC and TN and PACS-2 as standard material.

Samples for diatom analysis in the Laguna Cascada sediments were taken at every 2–3 cm and 65 samples were taken in the supposedly marine influenced sediments at Lago Galvarne Bog. The latter will not be published here as a diatom diagram but will mainly be used in the discussion on sea-level changes. All samples were first treated with 10% HCl, washed, and heated with 30% H_2O_2, at 80–90 °C for 2–3 h to remove organic matter. Then they were placed in a 100 ml beaker with distilled water for 2 h and decanted, and this was repeated until the water was transparent. Clay samples were washed repeatedly by suspending and dispersing the material in distilled water. The supernatant was discarded after 2 h. Permanent slides were mounted with Naphrax®. Diatom identification was made with a light microscope at 1000× magnification. The aim was to count at least 400 valves per slide, but in some cases this was not possible. The works by Hustedt (1930–1966), Cleve-Euler (1951–1955), Patrick and Reimer (1966–1977), Krammer and Lange-Bertalot (1986, 1988, 1991a,b), Round et al. (1990), Rumrich et al. (2000) were the main sources for species identification. The Tilia and TGview programs (Grimm, 1991) were used for plotting the diagram, where the species with more than 3% relative abundance in at least one sample are shown. Samples where the diatom sum was <150 were excluded from the percentage calculations. Diatom zonation was aided by the CONISS program (Grimm, 1991).

3.1. XRF analyses as paleoenvironmental proxies

Non-destructive X-ray fluorescence (XRF) analyses of the two sequences were performed using an ITRAX core scanner (Croudace et al., 2006) at Cox Analytical in Göteborg (Sweden). A molybdenum X-ray source was used which allows measurements of a wide range of elements. We selected 15 elements (Al, Si, P, S, Cl, K, Ca, Ti, Mn, Fe, Br, Rb, Sr, Pb, and Zr) for a more detailed analysis. The resolution of the scans was 1 mm with an exposure time of 1 s. The XRF data set was smoothed with a 10 point adjacent averaging to achieve better visibility, which means that intervals between each data point in the graphs correspond to 10 mm. The XRF scanning results represent relative counts and are displayed as counts per second (cps). Due to the detection limit, values below 50 cps must be interpreted with caution.

Pearson's correlation coefficients (Trauth, 2006) have been used to explore relationships between the different elements and these are presented as correlation matrices in supplementary Fig. S1. The XRF data was separated into three major groups: Lago Galvarne Bog-peat (LGB-P), Lago Galvarne Bog-lake (LGB-L) and Laguna Cascada (CAS) prior to statistical analysis. The fields of a correlation matrix represent Pearson's correlation coefficients for each pair of elements. To calculate reasonable significance limits for the correlation coefficients, the number of XRF sample points was reduced by a factor of 10 by linear interpolation based on the depth axis. The differences between

the respective correlation coefficients before and after interpolation were negligible. Based on a *t*-test and an *F*-test as described by Taubenheim (1969), the significance limit for the correlation coefficients of the interpolated data sets is ±0.10.

3.2. Radiocarbon dating

Macrofossil and bulk sediment samples for ^{14}C analyses (Table 1) were pre-treated and measured at the AMS Radiocarbon facility at Lund University. The radiocarbon dates were calibrated using the SHCal04 calibration curve (McCormac et al., 2004).

The age–depth relationship for each sequence is based on the assumptions that any significant changes in sedimentation/accumulation rate should occur at lithologic boundaries, and that peat or macrofossil dates are more reliable than bulk sediment dates. In addition, an age–depth model for each core was calculated with the OxCal 4.0 calibration software (Bronk Ramsey, 2001, 2008). This program combines the probability distributions of the calibrated radiocarbon ages with certain assumptions on depositional processes to obtain an age–depth curve with the 1σ probability margins of the radiocarbon ages. We chose to apply the *P_Sequence* model of OxCal 4.0 to our data which assumes deposition to be random (meaning no regular annual layers) but an approximate proportionality to the depth *z* is given (Bronk Ramsey, 2008). As a *k*-value, which gives an estimate of the variation from a constant sedimentation rate we chose 200, which is equivalent to 5 mm calculation increments. Thereafter we used an age–depth curve based on sedimentation changes at lithologic boundaries (thick black line in Figs. 3 and 6) to plot the proxy data of the cores discussed hereafter. Calibrated years are in the following denoted as cal BP (before AD 1950).

4. Results and discussion

4.1. Interpretations, comparisons and correlations of the geochemical data

Generally, the K and Ti content in lake sediments and peat can be used as a proxy for minerogenic deposition. In the analyzed sections K and Ti are strongly correlated ($r = 0.62$–0.80) in all three groups (supplementary Fig. S1A–C). In raised bogs, these elements mainly reflect atmospheric deposition of dust aerosols or tephras. Hence, they mainly serve as indicators for wind and storm activity, including tephra fall-outs, in ombrotrophic peat, while they indicate the varying minerogenic content in lake sediments. In our case the clastic sediments of the nearby Cape Colnett (Dalziel et al., 1974) and the dominating volcanic bedrock of Isla de los Estados can deliver the clay mineral illite ($[K,Ti]Al_3Si_7O_{24}$) as a source for the two elements. This is supported by a strong correlation of K ($r = 0.72$) and a less strong correlation of Ti ($r = 0.48$) to Si in the CAS record.

While K and Ti behave rather inert in an aquatic/wet environment, Ca is strongly influenced by the pH of the sediment as part of the carbonate cycle. It correlates very well with K and Ti in the CAS record ($r = 0.49$–0.70), where it most likely indicates minerogenic input with Ca-feldspar ($CaAl_2Si_2O_8$) as source mineral. In contrast Ca does not correlate with K and Ti in the LGB records, but shows a high correlation with S in the LGB-L sequence ($r = 0.65$), indicating marine influence.

Changes in Fe and Mn are more difficult to interpret (Engstrom and Wright, 1984) since a number of independent environmental factors control their supply and sedimentation. The Mn/Fe ratio is often used as an indicator for redox conditions (Davison, 1993). As Fe^{2+} is less stable in pore water than Mn^{2+}, it precipitates earlier than Mn^{2+} and hence the Mn/Fe ratios in the sediment are low when the sediment becomes anoxic (Koinig et al., 2003). However, the behavior of Mn also depends on pH, as Mn^{2+} mainly precipitates as $MnCO_3$. If the decomposition/humification rate increases, the consumption of oxygen also increases while pH decreases due to the release of CO_2. This leads to a mobilization of Mn^{2+} and to a decrease in the Mn/Fe ratio (Koinig et al., 2003). Furthermore, Mn and especially Fe have shown to be good indicators for marine–fresh-water isolations (Sparrenbom et al., 2006), possibly due to a flocculation effect when fluvial/fresh-water mixes with marine water (Sholkovitz, 1978). Fe correlates very strongly to K and Ti in the LGB peat ($r = 0.90$–0.86) and lake groups ($r = 0.78$) and moderately ($r = 0.46$–0.58) in CAS, suggesting similar chemical behavior during deposition.

Fe and Br show a correlation in the peat and lake sediment of the LGB core ($r > 0.5$), but no correlation in the CAS core ($r = -0.11$). Fe reduction takes place in the salinity transition zone between marine and fresh-water systems (Snyder et al., 2004), which partly explains the correlation between Fe and Br. Br is often used as a geochemical proxy for hypersaline lakes and playa salt deposits (Ullman, 1995; Risacher and Fritz, 2000) and is common as bromide salts in sea water, but it occurs in only extremely small concentrations in fresh-water systems (Song and Müller, 1993). Br is therefore a useful indicator for saline waters. Its dominant aqueous species, Br^-, shares many chemical characteristics with the abundant salt constituent chloride, Cl^- (Ullman, 1995). However, Cl counts in both cores are extremely low due to the XRF-scanning setup; hence no reliable conclusions can be drawn from this element record. Lago Galvarne Bog is located close to the sea and Br can thus be used as an indicator of direct influence of marine water. In the case of Laguna Cascada we assume that Br can be a proxy for marine aerosols, i.e. sea spray, which was transported from the coast to the site. Higher Br values should then indicate higher wind activity.

4.2. Lago Galvarne Bog (LGB)

The proximity to the sea makes this basin and its deposits sensitive to sea and base level changes, which is also shown by the transition from terrestrial deposits (peat) to aquatic sediments (gyttja) at 480 cm, dated to c. 8000 cal BP (Fig. 3). Hence, to understand the development of the basin it is important to recognize the relationship between sea level, thresholds—possibly comprised by beach ridges—and sedimentation in the basin. Today, the lake is dammed by a storm beach ridge and the lake and its peat land are drained through the

Table 1
List of radiocarbon samples taken from Lago Galvarne Bog (LGB) and Laguna Cascada (CAS) all samples calibrated with OxCal 4.0, all ages in 1σ range. (The sample numbers refer to the sampling depth before adjusting the field-based correlations between individual core sections in the laboratory. Magnetic susceptibility (κ) measurements which give a relative estimate of the magnetic mineral concentration aided the visual correlation between overlapping core segments.)

Sample no.	Analysis no.	Sample material	^{14}C age (BP)	1σ error (BP)	SHCal04[a]	Depth (cm)
LGB/31	LuS 6791	Peat	310	50	450–280	31
LGB/125	LuS 6512	Peat	1665	65	1570–1410	130
LGB/210	LuS 6792	Coarse detritus	3245	50	3460–3360	216
LGB/300	LuS 6509	Coarse detritus	3460	60	3820–3560	303
LGB/375	LuS 6793	Gyttja	4870	50	5610–5470	365
LGB/433	LuS 6794	Gyttja	6210	60	7160–6970	423
LGB/500	LuS 6511	Peat	7050	65	7930–7750	490
LGB/547	LuS 6795	Peat	8130	55	9120–8780	539
CAS/126	LuS 6929	Peat	1290	50	1256–1083	126
CAS/162	LuS 6506	Gyttja	2605	50	2748–2503	162
CAS/189	LuS 6930	Gyttja	2600	50	2746–2502	189
CAS/235	LuS 6931	Gyttja	4115	50	4785–4438	235
CAS/281	LuS 6932	Gyttja	5000	50	5720–5609	281
CAS/324	LuS 6933	Gyttja	5675	50	6445–6318	324
CAS/346	LuS 6934	Gyttja	5920	50	6775–6571	346
CAS/387	LuS 6935	Gyttja	7715	60	8537–8400	387
CAS/391	LuS 6936	Gyttja	7775	60	8548–8429	391
CAS/421	LuS 6937	Gyttja	9125	60	10283–10178	421

[a] Ages in cal BP; until 11.0 ka BP, based on McCormac et al. (2004).

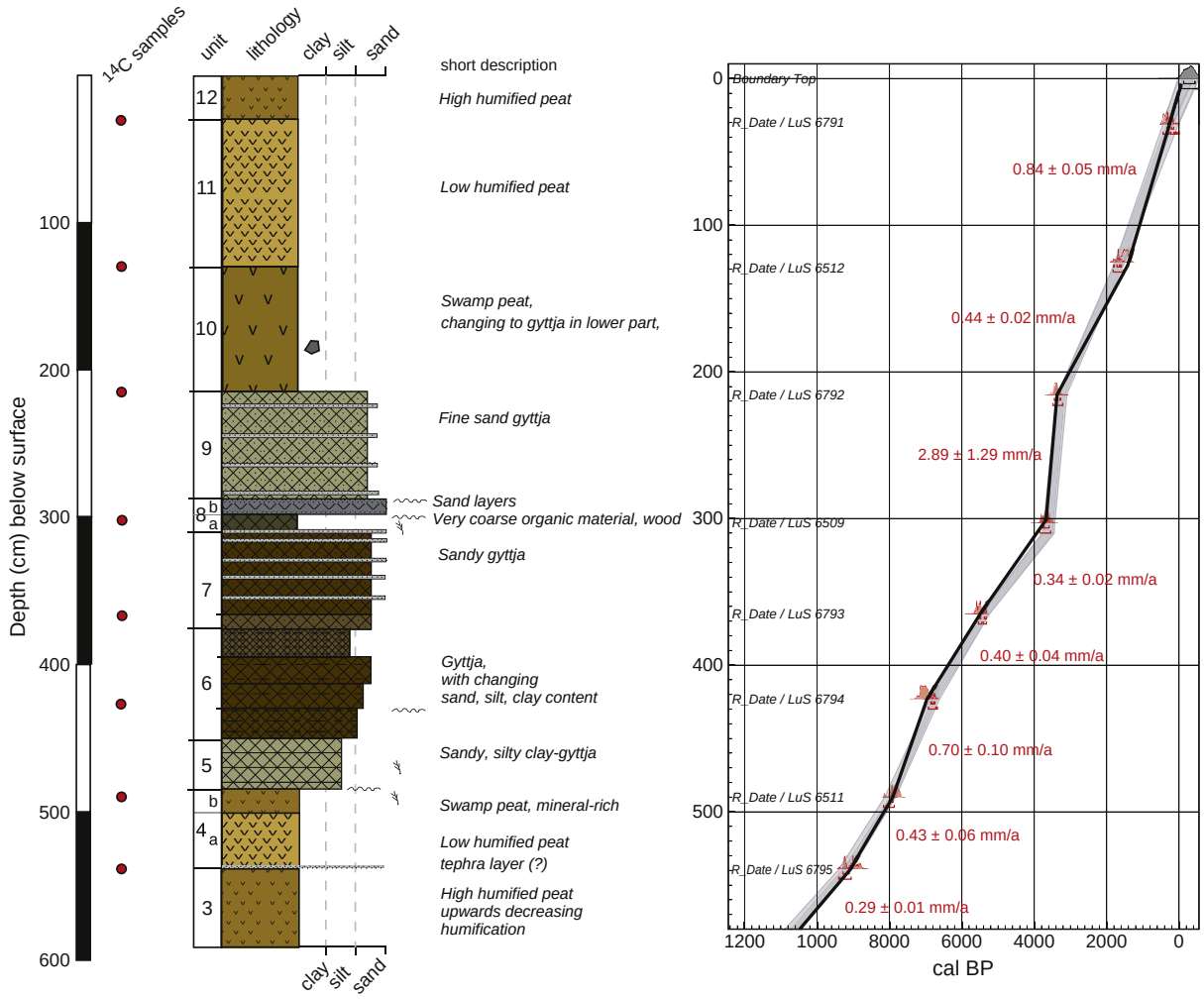

Fig. 3. Lithologic units and radiocarbon dates from Lago Galvarne Bog (LGB). The black line in the diagram to the right shows the lithology-based age–depth function. The light-grey area behind it shows the 1σ-range of the statistical age–depth model calculated with OxCal 4.0.

cobbles of the 10–20 m wide beach ridge in the northwestern corner of the lake. The area between the eastern–northeastern lake shore and the sea is made up by beach cobbles covered by peat. However, the position and configuration of the beach have possibly changed continuously during the Holocene. It is likely that beach ridges, and possibly also arched moraine ridges (Björck et al., 2007; Möller et al., 2010), often formed less protective thresholds for the basin than today's well-developed beach ridge. Our estimates of former sea levels are based on the assumption that the threshold, its altitude, and degree of protection have shifted with time and changing sea levels. Today the beach ridges at Bahia Colnett and at the former prison village in Bahia Cook, built in the late 19th century, are being eroded. This implies that the local sea level is presently rising, showing that the beach ridges are vulnerable to transgressions. Today's situation, with a damming beach ridge and a lake/bog level c. 2 m above mean sea level (c. 0.5–1 m above high tide level), is a good approximate boundary condition for pure limnic conditions, at least when the basin is protected by a well-developed beach ridge. If mean sea level would be higher than today, a period of storm events would most likely change the conditions inside the basin for a longer or shorter time; a single storm during the field work almost demolished and reworked parts of the beach that today functions as the threshold. To assess absolute past sea levels, i.e. in relation to today's sea level (=0 m), during, e.g., transgressions, we also have to consider depths below today's sea level for the studied sediments. When interpreting the sea-level changes the sediment depths will therefore be related to the present mean sea level, and the implications for this will be discussed in Section 4.2.2.

4.2.1. Lithostratigraphy and chronology

Since it was not possible to penetrate the corer further than 745 cm, we speculate that the cored sequence is underlain by stones or till. The stratigraphy between 745 and 537 cm (16100–9040 cal BP) has been described by Unkel et al. (2008). The sequence above 537 cm (<9040 cal BP), which was the focus of this study, shows a continuous record up to present and can be divided into 8 units, of which units 4 and 10–12 consist of peat with different degrees of humification. The gyttjas of units 5–9 (7885–3440 cal BP) reflect aquatic sedimentation and contain several layers of sand and coarse organic material (Fig. 3). The lithology is described in more detail in Table 2. Further information can be found in the online supplementary file to this paper.

4.2.2. Geochemistry and magnetic susceptibility with environmental implications, including salinity changes

The peat in units 3 and 4 has an organic matter content of 90–95% (Fig. 4) and is possibly formed in a transitional environment from bog to fen during the early Holocene. The upwards decreasing humification and increasing ash content indicate that the bog became more water-logged, which could have been caused by rising ground water, considering its coastal position possibly driven by rising sea level.

Table 2
Detailed lithostratigraphy of Lago Galvarne Bog (LGB). Note that Fig. 4 is the log version of this table and that units 1–8 have been described earlier by Unkel et al. (2008).

Unit #	Depth (cm)	Lithologic description
12	30–0	Highly humified water-logged peat.
11	130–30	Peat, low humified.
10	216–130	Swamp peat. An angular pebble clast occurs at 184–181.5 cm.
9	287–216	Fine sandy gyttja. A cyclic sedimentation of coarse detritus and sandy layers with at least 28 such layers.
8a	310–297	Sandy coarse detritus gyttja with wood pieces up to 5 mm in size and possibly also marine macro-algae.
b	297–287	Four sand layers, each 0.5–2 cm thick, separated by thicker layers of coarse organic matter. The upper boundary is very sharp.
7	377–310	Sandy gyttja, composed of alternating layers of coarse and fine detritus gyttja, with several intercalated distinct sand layers.
6	450–377	Gyttja with varying content of sand, silt and clay
5	485–450	Sandy to silty clay gyttja, fairly rich in coarse plant remains
4a	537–502	Low humified peat, incl. a thin sand layer with grain sizes of 1–2 mm.
b	502–485	Swamp peat, rich in macro-fossils and mineral grains.

The transition into the swamp peat of unit 4b (8225 cal BP), displayed by significantly lower LOI values, high magnetic susceptibility and high K, Ti and Fe values (Figs. 4 and 5), shows that the ground water level/base level had risen notably, and had flooded the fen. This flooding could partly be related to increased surface run-off as a consequence of increased precipitation, as shown by the

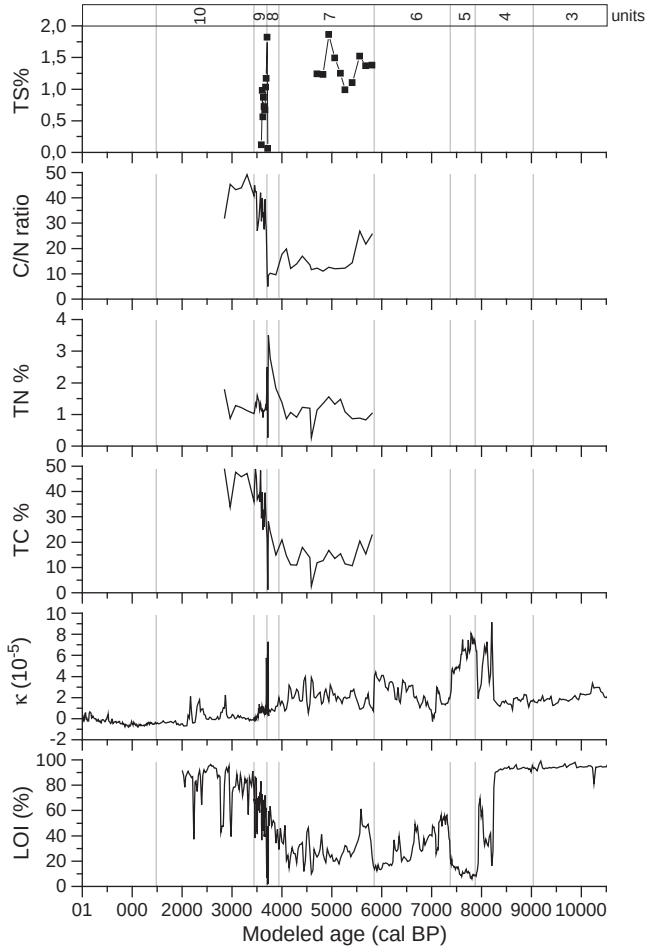

Fig. 4. Loss on ignition (LOI), magnetic susceptibility (κ), total carbon (TC), total nitrogen (TN), carbon/nitrogen ratios (C/N) and total sulphur (TS) measurements from Lago Galvarne Bog (LGB). TC, TN and TN were only analyzed on selected units. The lithologic units as described in the text are shown to the right.

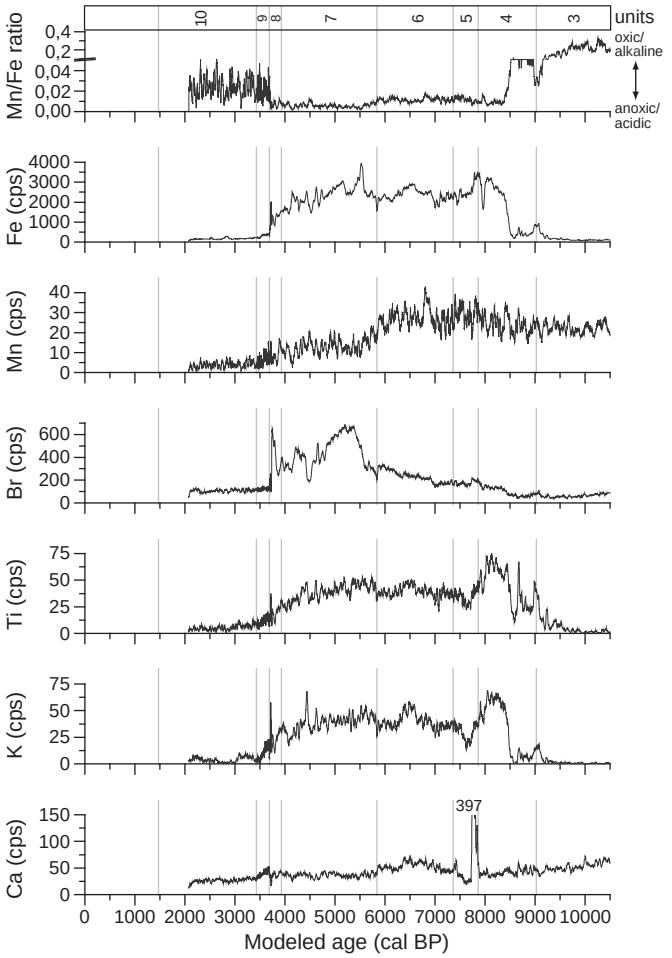

Fig. 5. XRF measurements of the elements calcium (Ca), potassium (K), titanium (Ti), bromine (Br), manganese (Mn) and iron (Fe), and Mg/Fe ratios from Lago Galvarne Bog (LGB) plotted against age (cal BP). The lithologic units as described in the text are shown to the right.

abundance of coarse mineral and organic particles, but was most likely also a result of an approaching sea level and a rising ground water table, but without a direct impact of marine waters. This assumption could consequently give a hint of the altitude of the local sea level at that time. Since the lithologic change from unit 4a to unit 4b occurs at 5 m below lake level, which is 3 m below present mean sea level (−3 m), and if we regard today's situation with a lake 2 m above mean sea level as a rough altitudinal limit for maintaining a fresh-water environment, sea level at 8200 cal BP was probably situated at least below −5 m, but possibly not much lower (Fig. 6). An intriguing feature is also the onset of rising K, Ti and Fe values (Fig. 5) already in unit 4a at 9000 cal BP. This might represent the first stage of the flooding of the peat land, but could partly also have been caused by increased deposition of aeolian sediment and aerosols as the beach came closer with the rising sea level. Gradually increasing Br values after 8500 cal BP can be explained by increased deposition of marine aerosols from sea spray.

The clay gyttja of unit 5 (7885–7455 cal BP) shows that the site had now become part of a water-filled basin with fairly rapid sedimentation of dominantly mineral material. In fact, organic matter displays a minimum (12%) in this unit, while magnetic susceptibility attains a maximum coinciding with a distinct maximum in Ca at 7780 cal BP (Figs. 4–5). The K and Ti records decrease clearly to lower levels, which may be related to a change in the sediment source, while Br and Fe counts are stable. Marine and brackish diatoms are fairly common from the onset of this unit, which shows that sea level was

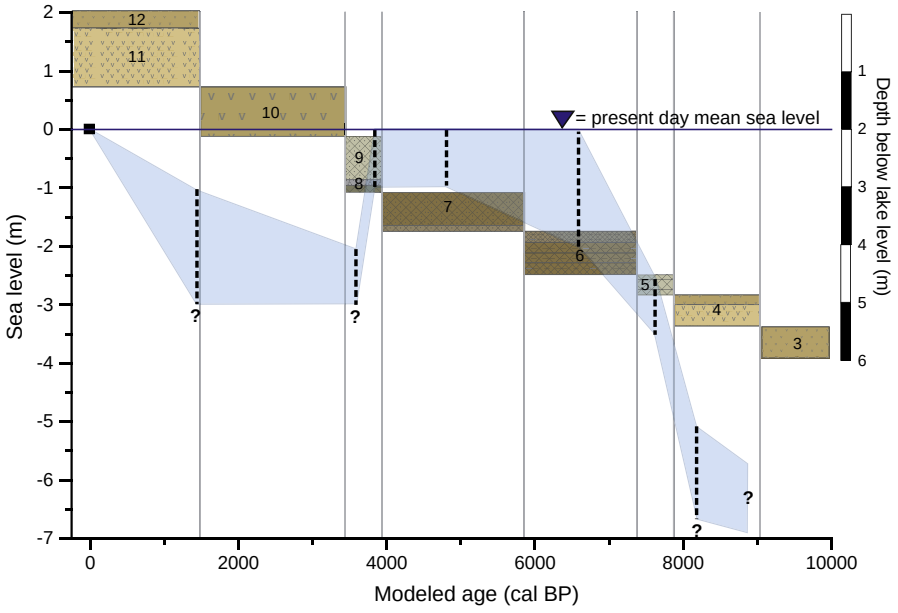

Fig. 6. Graph showing the interpreted sea-level development in the study area during the Holocene as inferred from the Lago Galvarne Bog record. To the left, the sea level is given in meters below or above present day mean sea level, and to the right, the relative sediment depth in relation to the present day lake level is shown. This clarifies how the absolute sea levels were reconstructed by combining estimated marine influence with sediment depth in relation to present day mean sea level. The black dotted lines within the different units reflect a subjective uncertainty of our reconstruction, based on the possible sea-level range of c. 1–2 m on the *x*-axis. The light blue band illustrates the uncertainty range of a "sea-level curve" by simply connecting our estimated levels. The lithologic units in the background (numbered 3 to 12) are shown in correct depth scale as used in Fig. 3, covering the time periods of their formation, cf. *x*-axis.

approximately at the sill of the basin, with at least a distinct marine influence during high tide. This unit is found at c. −2.5 m and we set mean sea level at c. −3 m.

The gyttja of unit 6 (7455–5880 cal BP) is characterized by a highly variable organic content (15–50%), which decreases upwards leading to minimum values at the top of the unit. As would be expected, this trend is opposite to the magnetic susceptibility record. With the exception of the steadily rising Br values the XRF data show no distinct changes or clear trends. The Br and Fe data, in combination with higher minerogenic content, imply gradually increasing marine influence, probably as an effect of rising sea level and increasing impact of storms and maximum high tides. Diatom analyses imply the largest marine influence at the sediment depth of 4 m, corresponding to c. 6500 cal BP, with species such as *Gyrosigma nodiferum* (Grunow) Reimer, marine *Paralia* sp. and *Cyclotella striata* (Kützing) Grunow. The basin had probably turned into a lagoon already before with more or less enclosed estuarine conditions. Depending on how well-protected the basin was, salinity may have changed over time. At 6500 cal BP mean sea level had possibly risen to, or even above, the sill (Fig. 6), and since this sediment level is found at −2 m, we estimate mean sea level to c. −2 to 0 m.

The onset of unit 7 (5880–3940 cal BP) is marked by a rise in organic matter (50–60%) lasting for c. 500 years, followed by values of 20–30%, where several sand layers show up as minima in organic matter and peaks in magnetic susceptibility. The C/N ratios are between 20 and 25, but later decline to 10–15 (Fig. 4). After the initial peak in organic matter both Br and Fe rise to clear maxima between 5400 and 5000 cal BP, while K and Ti slowly decrease towards the top of the unit. We interpret the highly organic and aquatically dominated material in the lower part of unit 7 as estuarine sediments with both fresh and marine water influences, which is supported by the diatom analyses. The deposits were possibly formed in a sheltered lagoon, with varying marine impact: the basin/lagoon may have been protected by a beach ridge, but due to storms this protection could have been damaged now and then. Although this would have resulted in more marine influence, as implied by the Br peak (Fig. 5) and increased deposition of sand (Figs. 3 and 4), the influence of fresh-water would still be significant. Since we think that the changing marine influence was more an effect of protection of the basin than changes in sea level we assume that sea level was approximately the same as in the preceding unit. Sea level should have been higher than the level of unit 7, −1.7 to −1.1 m, but not much higher due to the fairly large fresh-water influence. A conservative estimation is that mean sea level was situated between 0 and −1 m (Fig. 6).

Units 8 and 9 were deposited very rapidly and only cover 500 years in total (3940–3440 cal BP). The 23 cm thick unit 8 displays highly variable organic and minerogenic contents, with high Br and Fe counts and low C/N ratios, ending with sediments dominated by sand. Furthermore, unit 8 displays a maximum in marine diatom types. In contrast, the homogenous unit 9 has a high organic content (40–65%), high C/N ratios and low Br, Fe and susceptibility values. The boundary between units 8 and 9, situated at −0.8 m, is therefore an indication of a significant change in depositional environment, which is also displayed by the rapidly falling sulphur values.

We regard unit 8 as the end of any direct marine effect of the basin, which is supported by the diatom analyses: unit 9 only contains fresh-water diatoms. Unit 8b, with its distinct sand layers, may in fact represent the final transgressive and furthest inland phase of the raised beach ridge system that borders the basin today in the northeast, and at the onset of this subunit mean sea level would probably have been situated at or slightly above −0.8 m, i.e. at c. −1 to 0 m, indicating a more or less stable sea level since 6500 cal BP, with a dynamic estuarine environment at the site for more than 3000 years. Unit 9, situated at −0.8 to −0.1 m, is interpreted as a lacustrine sediment and is possibly the result of the establishment of a well-developed beach ridge system between the basin and the sea. The high sedimentation rates may indicate that the basin was dammed up and now functioned as a trap for water-transported sediments from areas further inland. With the sharp transition from the marine influenced unit 8 into the fresh-water unit 9 we think it is most likely that sea level had begun to drop in the top of unit 8 and was at least situated below −2 m at the onset of unit 9.

Unit 10 (3440–1485 cal BP) displays a transition into limnic/terrestrial deposition; while the lower part is a gyttja-like peat the

upper part is a swamp peat. This is also implied by the high C/N ratios in the lower part grading into lower ratios after 3000 cal BP. The swamp peat is usually highly organic (80–90%), but thin and distinct layers of mineral matter also occur, indicated by susceptibility peaks (Fig. 4). In this upper part all the mayor element records reach very low values. At 183 cm core depth (c. 2670 cal BP) a 2.5 cm large rock clast was discovered in the peat, the origin of which is not clear. While the thin horizons of mineral matter may be interpreted as being of aeolian origin from the close-by beach, a clast of such size could not have been wind transported, but rather by another agent such as ice or birds. The transition from lake sediment to peat, between −0.1 and 0.7 m, is the end of aquatic influence and indicates a lowering of relative base (sea) level. Since the sedimentation and overgrowth raised the surface of the bog, a further large sea-level lowering is not necessary for explaining this change. We therefore estimate that sea level was at least situated below −1 m at the transition between units 10 and 11, dated to c. 1500 cal BP (Fig. 6).

Units 11 and 12 were not geochemically analyzed, but they form a natural continuation of lake overgrowth and peat accumulation. We speculate that the whole basin was covered by peat during the peat growth of units 10 and 11. One likely explanation for today's open water in the eastern part of the basin is a sea-level transgression causing a rising ground water level in the basin. For example, an extreme storm event could have resulted in (a fairly recent) destruction of the damming and very narrow beach ridge. This would have opened the basin for eroding sea waves as well as through-flow of fresh-water via any opening in the beach ridge. This is supported by depth soundings carried out in the lake, which show the presence of a 2.5–2.8 m deep channel slightly east of the bog and directed towards the northwest where the narrowest part of the beach ridge occurs today. Tidal effects could have amplified the erosion of the peat land. Later, the beach ridge must have closed, possibly by re-establishment of the protecting beach. When this happened is not known, but the ongoing transgression and coastal erosion indicate that it might have been a fairly recent event.

4.3. Laguna Cascada

4.3.1. Lithostratigraphy and chronology

The lower part of the Laguna Cascada sequence, between 523 and 421.5 cm, consists of eight lithological units dated to ca. 16200–10600 cal BP (Unkel et al., 2008). The upper part between 421.5 and 80 cm is divided into units 9 to 20 and covers the remaining part of the Holocene (Fig. 7; Table 3). In the following, we present some highlights of the lithology of the Laguna Cascada core. A more detailed description is given in Table 3 and in the online supplementary file to this paper.

The transition from the deglacial-early Holocene part of the sequence into unit 9 (421.5–391 cm; 10600–8775 cal BP), a silty and algae-rich detritus gyttja with ~20 fairly thick dark laminae (Fig. 7), is sharp but without signs of erosion.

Unit 10 is most likely a 2.5 cm thick tephra layer, with a greenish colour and fine sandy–silty grain size. Samples for ^{14}C dating directly above and below the unit (LuS 6935 and LuS 6936, Table 1) yield nearly the same age of 7775 ± 60 ^{14}C yr BP and 7715 ± 60 ^{14}C yr BP, respectively (8548–8400 cal BP). The tephra could correlate to the H_1 eruption of the Hudson volcano in Chile (45°54′S, 72°58′W), dated to 8417–7624 yr cal BP by Kilian et al. (2003). Stern (2008) also describes the H_1 tephra as green, which distinguishes it from the white and slightly older MB_1 tephra from Mt. Burney and notes that this eruption has been found on Isla Grande Tierra de Fuego with a thickness of more than 15 cm.

The rather constant sedimentation of units 9–13 is sharply interrupted at 345 cm, probably as an erosion discordance, by the diamict sediment of unit 14, which was deposited fairly rapid, as indicated by the ^{14}C dates directly below and above the unit (LuS 6934

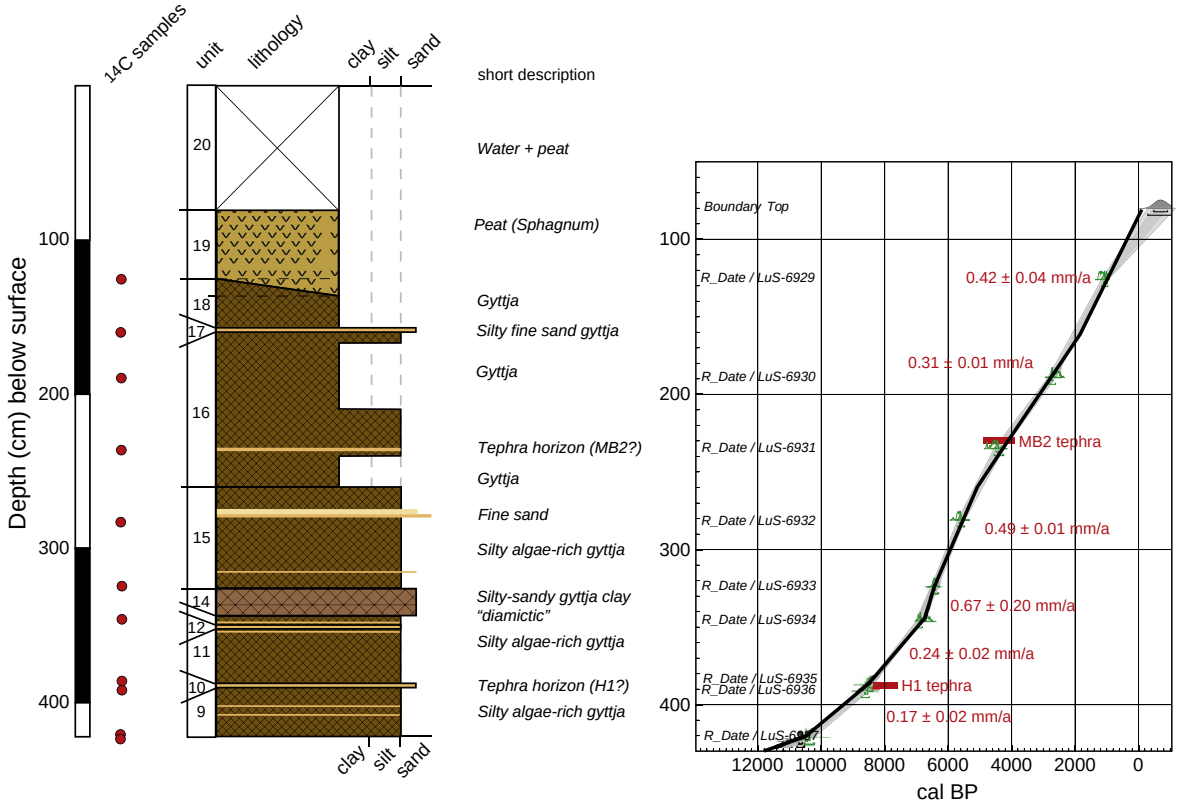

Fig. 7. Lithologic units and radiocarbon dates from Laguna Cascada (CAS). The black line in the diagram to the right shows the lithology-based age–depth function. The light-grey area behind it shows the 1σ-range of the statistical age–depth model calculated with OxCal 4.0.

Table 3
Detailed lithostratigraphy of Laguna Cascada (CAS). Fig. 8 is the log version of this table. Units 1–8 have been described earlier by Unkel et al. (2008). UB = upper boundary.

Unit #	Depth (cm)	Lithologic description
20	80–0	Mix of water and peat
19	137–80	Brown peat with a gradual gyttja-peat transition in the lower 10 cm.
18	157–137	Brown coarse detritus gyttja. UB = very gradual
17	161.5–157	Grayish-light brown silty-fine sand gyttja. UB = sharp
16	260–161.5	Brown-dark brown gyttja with higher algae and silt content between 240 and 210 cm. At 235 cm a 0.5 cm thin light brown silty layer occurs, possibly a tephra. The uppermost 30 cm is richer in coarse detritus. UB = sharp
15	325–260	Dark brown silty algae-rich gyttja with a 1 mm thin sand layer at 317.5 cm. At 279.5 cm a light-grey 0.5 cm medium sand layer occurs followed by 4 cm of brownish-grey clayey, sandy silt gyttja ending with a thin grey layer at 275 cm. UB = very gradual
14	345–325	Silty–sandy gyttja clay, "diamictic", with gravel clasts and organic lenses. UB = sharp
13	352.5–345	Dark brown silty algae-rich gyttja with one light layer at 349 cm. UB = very sharp and possibly erosive.
12	354.5–352.5	Light grayish-brown silty gyttja, which starts and ends with distinctly light layers (tephras?). UB = very sharp
11	388–354.5	Dark brown silty algae-rich gyttja, thickly laminated with more coarse detritus above 378 cm. At 360 cm a 0.5 cm light layer occurs. UB = sharp
10	391–388.5	Greenish sandy silt, possibly a tephra. UB = very sharp
9	421.5–391	Brown silty, algae-rich fine detritus gyttja. UB = very sharp

and LuS 6933; Table 1). The age–depth graph depicts an age of 6775 to 6465 cal BP for unit 14. This is, however, possibly an overestimation since the lithology of unit 14 suggests deposition as a sediment gravity flow, which may represent only one short event.

Gyttja sedimentation continues in units 15 to 17 (325–157 cm; 6465–1760 cal BP) At 235 cm a c. 0.5 cm thick light brown, silty layer occurs, which is tentatively interpreted as a tephra (Fig. 7). The ^{14}C sample taken directly below this layer at 235 cm depth, gave an age of 4115 ± 50 ^{14}C yr BP (4785–4438 cal BP). This age is close to that of the MB_2 eruption of Mt. Burney in Chile (52°20′S, 73°24′W), which has been dated to 4860–3900 cal BP by Kilian et al. (2003). Stern (2008) showed that the plume of the MB_2 eruption had a more south-easterly direction as compared to the MB_1 eruption, resulting in an often more than 1 cm thick tephra layer on Isla Grande Tierra del Fuego. Hence, the deposition of some millimetres thick layer on Isla de los Estados does not seem implausible.

Unit 18 (157–127 cm; 1760–1050 cal BP) is a brown silty gyttja gradually changing into a coarse detritus gyttja towards the top of the unit. The uppermost 10 cm forms a gradual transition from gyttja to peat and it is difficult to determine a clear boundary towards the overlying low humified *Sphagnum* peat of unit 19. This peat is 47 cm thick (127–80 cm; 1050 cal BP–present) and is covered by water and living *Sphagnum* moss in the form of a partly floating quagmire.

4.3.2. Diatom stratigraphy and environmental implications

The diatom stratigraphy displays three distinct diatom zones, Zones I–III, of which two can be subdivided into two subzones (Fig. 8).

Zone I: 422–400 cm (10670–9300 cal BP). The zone displays the dominance of *Aulacoseira* taxa (including *A. alpigena*, *A. distans*, *A. laevissima*, *A. ambigua*, *A. subartica*, and *A. tethera* Haworth). Normally, *Aulacoseira* spp are tychoplanktonics, often found in oligotrophic waters of high latitude areas and also in well mixed waters (Krammer and Lange-Bertalot, 1991a). Around this time, the deglacial conditions had ceased at the locality and the diatom assemblage shows a distinct lacustrine environment. However, in the lower part of this zone we see markedly increasing values of *Brevisira arentii* (Kolbe) Nagumo and Kobayashi (1977). This species is common in acid and dystrophic to mesotrophic lakes (Krammer and Lange-Bertalot, 1991a) and has also been found in shallow turbid lakes on the Malvinas/Falkland Islands (Flower, 2005). Furthermore, *B. arentii* has a highly disjoint distribution in both hemispheres (Flower, 2005) and is associated with high concentrations of dissolved organic carbon (DOC) in the water column (Köster and Pienitz, 2006). Higher DOC concentrations can be produced by late ice-out and higher precipitation (Pace and Cole, 2002) and also by in-wash from peat in the catchment (Dillon and Molot, 1997; Pienitz and Vincent, 2000). Also, *Stauroforma exiguiformis* (Lange-Bertalot) Flower (2005), an acidophilous species occurring mainly in water bodies and sometimes on wet places (Van Dam et al., 1994), reaches values of 20%.

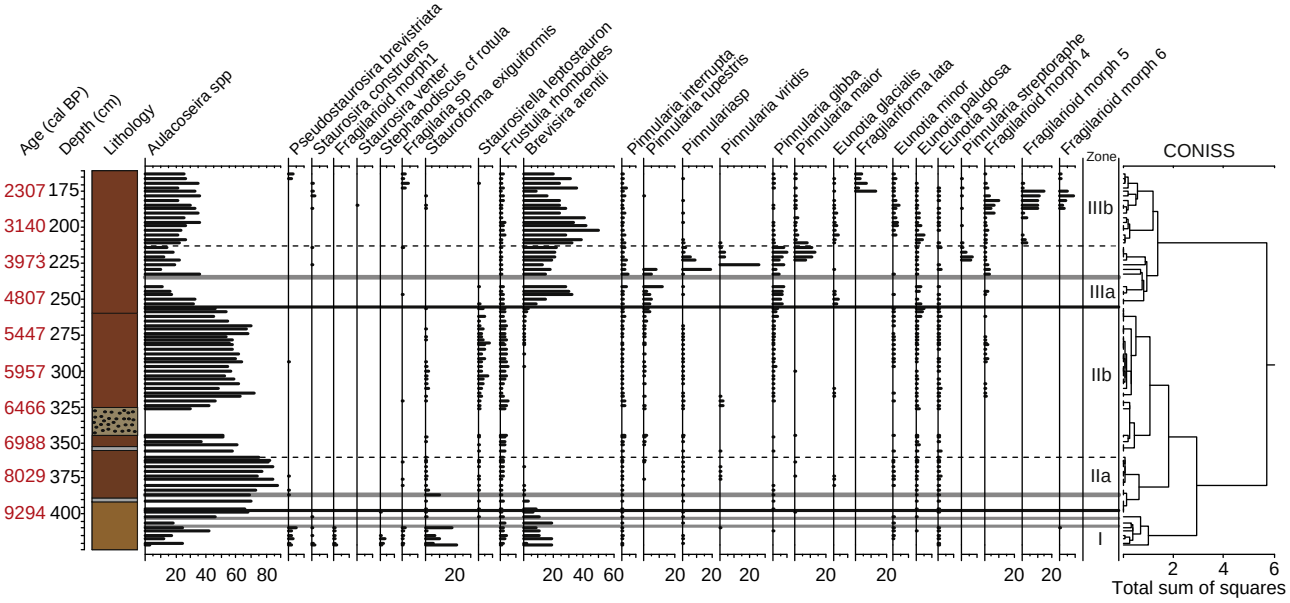

Fig. 8. Laguna Cascada diatom stratigraphy and CONISS cluster analysis. The species with more than 3% relative abundance are plotted. The shaded lines indicate assumed tephra layers. Three main diatom zones are shown in the graph.

In general, the diatom assemblage implies a distinct change in the development of Laguna Cascada, and may reflect the onset of a gradually more waterlogged and peat-rich environment around the lake. The co-dominance of *Aulacoseira* spp, *B. arentii* and *Staurofoma exiguiformis* indicates more acidophilous conditions in the water mass.

Zone II. This zone represents the most "pure" limnic stage of Laguna Cascada. The principal taxa are still *Aulacoseira* spp.

Subzone IIa: 400–360 cm (9300–7400 cal BP). The onset of this zone is characterized by the disappearance of *B. arentii*, and a notable increase of *Aulacoseira* spp. The latter reaches its highest percentage (85%) in this zone (Fig. 8). The reason for its extremely high abundance may partly be related to the presence of the thick tephra at 390 cm, possibly the H1 eruption from the Hudson volcano, providing extra silica for the bloom of this heavily silicified diatom type. It is known that tephra fall-out can produce changes in diatom communities or may produce blooms due to increased silica availability, water chemistry and turbidity (Harper et al., 1986; Abella, 1988; Birks and Lotter, 1994; Lotter et al., 1995; Telford et al., 2004). Furthermore, *Aulacoseira* spp are centric diatoms that need water turbulence and/or high water levels to remain suspended in the water column (Köster and Pienitz, 2006). Hence, the diatom record would support windier conditions at 8150 and 7500 cal BP as suggested also by the maxima of Bromine at this time. The dominance of this particular diatom indicates higher water levels.

Subzone IIb: 360–255 cm (7400–4975 cal BP). This subzone is interrupted by the unconformity at 345 cm and the diamict sediment of unit 14, but continues at 325 cm. The main taxa in this zone are *Aulacoseira* spp (75–85%) which implies higher lake levels, possibly as a result of more humid conditions. The *Pinnularia* group (*Pinnularia interrupta* W. Smith, *P. rupestris* Hantzsch, *P. gibba* Ehr) also contains benthic species which commonly occur in acidic environments, such as damp surfaces and peat bogs (Sterken et al., 2008). Oligothropic–dystrophic environments are indicated by the benthic *Eunotia* species. Overall this indicates increased acidic conditions, possibly as a consequence of higher precipitation and surface run-off from acid soils and weathered bedrock.

Zone III. Distinct changes in the diatom spectrum of Laguna Cascada occur in this zone. The development of the lake turned into a lake surrounded by peat land. The diatom diversity association suggests changes in climatic conditions and also implies changes in trophic levels. This may be the result of lower precipitation and weaker winds also shown by the geochemical analysis and the magnetic susceptibility. Thus, more periphitic life forms become more frequent, which may be linked with a further vegetation development of the area.

Subzone IIIa: 255–214 cm (4975–3600 cal BP). This subzone is mainly characterized by a significant decrease in planktonic species (*Aulacoseira* spp) and increasing abundance in *Brevisira arenti* (c. 35%). Species common in peat bogs such as *Pinnularia gibba*, *P. interrupta*, *P. maior* (Kützing) Rabenhorst, *P. rupestris*, *P. viridis* (Nitzsch) Ehrenberg, and *P. streptoraphe* Cleve become important at the end of this subzone. The association of this diatom flora may indicate a lake level lowering and the onset of peat overgrowth around the lake margin.

It is notable that *Aulacoseira* spp reached peak values immediately after the assumed Mt. Burney MB_2 (Stern, 2008) tephra deposition at 235 cm (Fig. 8), which together with distinct peaks of many *Pinnularia* species would imply that lake chemistry changed coincident with the tephra fall-out.

Subzone IIIb: 215–160 cm (3600–1830 cal BP). B. arentii reaches its highest percentages (40–50%) in this subzone, while *Aulacoseira* spp values are at 30–40%. The generally high abundance of *B. arentii* indicates more acid conditions. Apart from these two dominating types; *E. paludosa* and *E. minor*, which indicate oligotrophic conditions; Fragilarioid morphs 4, 5, and 6 are the most common species with no environmental information available. At the top of the sequence *Fragilariforma lata* (Cleve-Euler) Williams and Round becomes important. This species was recorded on a pond with a pH 5.4 at Malvinas/Falkland islands (Flower, 2005). Also, it is present in oligotrophic, circumneutral to acid environments (Kilroy et al., 2003). The number of species associated with peat environments increases upwards and dominates the end of the zone. This is most likely related to overgrowing of the fringes of the Laguna Cascada basin. Therefore, it may be the time when the shallow parts of the lake started to become a real peat bog. The amount of species associated with peat environments dominates at the end of the sequence. The environmental development at Laguna Cascada seems to have clearly changed from pure limnic conditions (Zones I and II) to an environment heavily influenced by peat lands (Zone III).

4.3.3. Geochemistry and magnetic susceptibility with environmental implications

The TC in the gyttja of unit 9 (10600–8675 cal BP) increases gradually from 11 to 21% (Fig. 9), parallel to an increase in the C/N ratio from 19 to 27. A peak in Fe occurs between 10000 and 9500 cal BP together with a smaller peak in the Rb/Sr ratio. Magnetic susceptibility, Ca, K, Ti, Zn and Sr display distinct peaks at the onset of unit 10 (Fig. 10). We regard this as the elemental signal of the

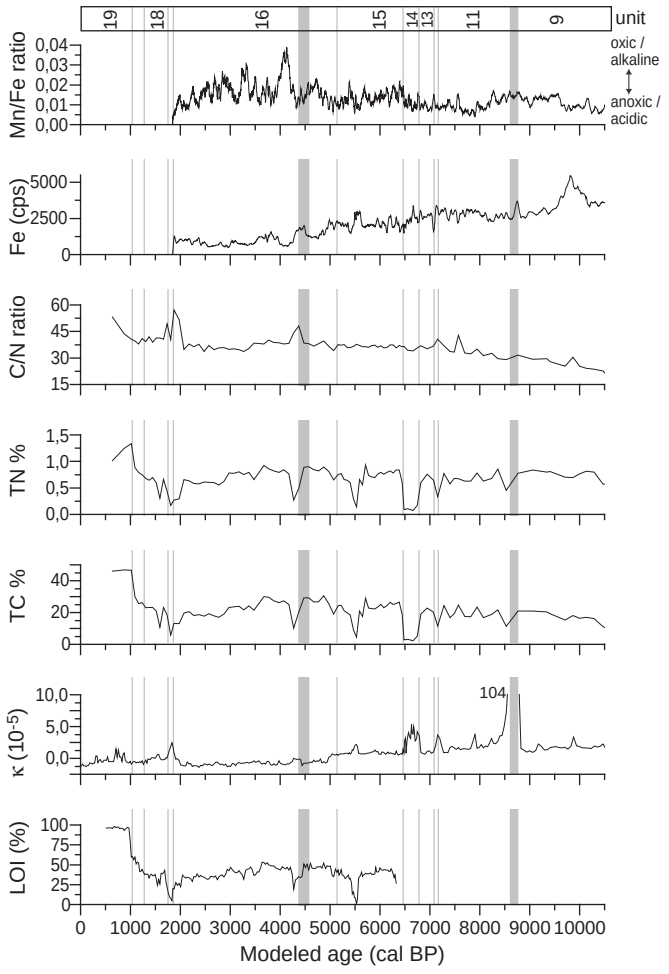

Fig. 9. Loss on ignition (LOI), magnetic susceptibility (κ), total carbon (TC), total nitrogen (TN), carbon/nitrogen ratios (C/N), XRF measurements of iron (Fe) and Mg/Fe ratios from Laguna Cascada (CAS) plotted against age (cal BP). The lithologic units described in the text are shown to the right and the two most prominent tephra layers, tentatively correlated to the H_1 (ca. 8500 cal BP) and the MB_2 eruption (ca. 4500 cal BP), are shown as grey bars.

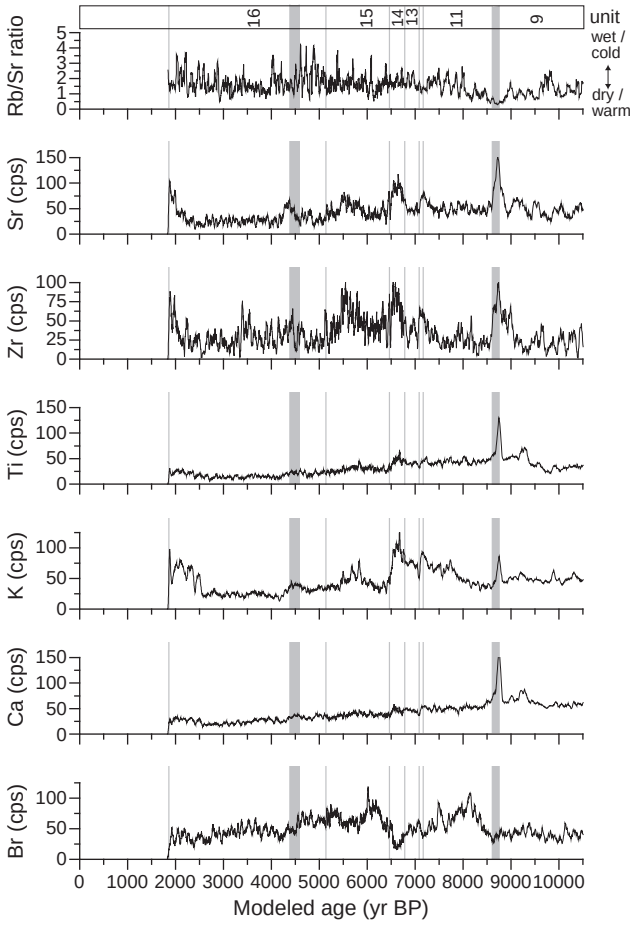

Fig. 10. XRF measurements of the elements bromine (Br), calcium (Ca), potassium (K), titanium (Ti), zirconium (Zr), strontium (Sr) and Rb/Sr ratios from Laguna Cascada (CAS) plotted against age (cal BP). The lithological units are shown to the right, including the two tephra layers as shown in Fig. 9.

2.5 cm thick tephra, which we tentatively assign to the H_1 tephra. Since no samples were analyzed for TC and TN in the very tephra, the response in these records is only seen just above the tephra layer at 387 cm, in the bottom part of unit 11, where their respective values drop to half of the previous values.

After the tephra peak, records of Ca, Ti and Fe show a common trend of continuous decrease throughout unit 11, while Br has two maxima around 8150 and 7500 cal BP. This might indicate periods of more windy conditions.

Minor peaks in K, Zr, Sr and magnetic susceptibility, dated to ca. 7150 cal BP, as well as minima of TC and TN, characterize unit 12. These features in combination with the occurrence of thin silty light-grey layers make it likely that the unit is a tephra horizon. With respect to lithology and geochemistry unit 13 (7100–6775 cal BP) is a continuation of unit 11 after the interruption of the tephra influenced sediment of unit 12.

The diamict sediment of unit 14 shows up as a prominent peak in the K, Zr and Sr record, while Fe, Ti and Ca show no response in this anomalous sediment unit. TC and TN fall to their lowest values since deglaciation, clearly showing that the unit is mainly built up of minerogenic, possibly terrigenous, material, with the exception of some large clasts and lenses of organic detritus. We interpret this unit as a sediment gravity flow, possibly as an effect of increased surface run-off during more humid conditions.

In unit 15 (6475–5140 cal BP), Br rises to another maximum at c. 6000 cal BP. This possibly reflects more windy conditions resulting in higher aerosol input. After this peak Br gradually decreases, with some minor fluctuations, until the top of unit 16. Zr counts are still high and Sr and K values are lower than in unit 14, but still relatively high. C/N ratios are constant throughout the unit, with the exception of a sand layer at c. 5500 cal BP which results in the TC, TN and LOI minima.

With the exception of the uppermost part, the fairly complex unit 16 is characterized by relatively low (and decreasing) XRF counts, and high and stable C/N ratios (between 35 and 40). The latter indicates a strong terrestrial component in the organic bulk material, which rises gradually throughout the sequence. The only exception from these trends is the minerogenic layer at 234 cm, displayed by Sr and Fe peaks and C and N minima, possibly caused by the MB_2 eruption. This is followed by a prominent peak in the Mn/Fe ratio and may reflect a short term change to more oxic and/or alkaline conditions in the lake. In general unit 16 shows stable conditions for more than 2500 years until about 180 cm (2500 cal BP), when K, Sr and Zr start to rise followed by a peak in C/N ratios. This implies lower lake levels ending up with the sand of unit 17, dated to c. 1800 cal BP; the sand and the very high C/N ratios imply that the lake shore was closer to the site.

The uppermost part of the core, corresponding to units 18 and 19, could not be analyzed by XRF scanning due to the fluffy structure of the organic sediment, but the lithology, grading from sand into coarse detritus gyttja, tells us that the lake level most likely rose again and C/N ratios are as expected high. The overlying peat, unit 19, shows that the overgrowth of the lake began at c. 1000 cal BP.

5. A paleoenvironmental and paleoclimatic synthesis

The two sites that we have investigated have been impacted by two very different forcings during the Holocene. While Laguna Cascada (CAS) and its sediments have been directly influenced by changes in the regional climate regime, mainly governed by the changing strength and position of the Southern Hemisphere Westerlies (SHW), the location of Lago Galvarne Bog (LGB), behind a dynamic beach, means that the sediment history of the basin is closely related to effects of local relative sea-level changes. We will therefore focus our discussion on these two topics.

5.1. Holocene variations of the SHW

In this paragraph, we use the sediment lithology, diatom stratigraphy and geochemistry from CAS as the main paleoclimatic proxies.

Br counts in the CAS sediments increase at 8500 cal BP and remain high until about 4500 cal BP, with two distinct peaks around 8000 cal BP and 6000 cal BP. Br occurs in fresh-water lakes and streams in very low concentrations (Song and Müller, 1993), and its most likely source are marine aerosols, which are high in bromide salts during periods with stronger or more frequent storms. The same interval is also characterized by high K, Ti, Zr, Sr and Fe counts, which were most likely caused by higher deposition of minerogenic matter from the catchment by surface run-off and streams. Higher magnetic susceptibility and slightly lower organic matter content could support this assumption. Moreover, the diatom assemblages (mainly Zone II) imply increasing and persistently high lake levels and surface run-off. All in all, the different records indicate increased windiness, increased precipitation and higher surface run-off between 8500 and 4500 cal BP.

The climate of Isla de los Estados is dominated by the effect of the SHW, which brings most of the precipitation. Changes in precipitation and windiness on Isla de los Estados are therefore primarily driven by changes in the strength and/or position of SHW. Our data indicates that the SHW intensified at 54°S between 8500 and 4500 cal BP, as a consequence of a more poleward position or a general strengthening/focusing of the SHW.

A similar pattern in the development of the SHW has been inferred at many sites in southern South America. Based on changes in precipitation patterns inferred from a marine sediment core off the coast of Chile at 41°S, a poleward displacement of the westerlies between 7700 and 4000 cal BP, with a peak of the change between 6000 and 5300 cal BP, has been reported (Lamy et al., 2001). At Lago Cardiel at 49°S increased wind speeds at c. 6800 cal BP have been inferred from wind-induced lake-water current proxies (Gilli et al., 2005). A more northerly position (49°S) of the SHW at this time would also explain a weakening of the SHW over Isla de los Estados (54°S) as expressed in our Br minima after 7000 cal BP. In contrast to this, Huber et al. (2004) report increasing *Ericacea* pollen between 6000 and 5000 cal BP from Haberton Bog in the Beagle Channel at 54°S and high, but variable, charcoal accumulations in South Patagonia and Tierra del Fuego during the first half of the Holocene, which are often interpreted to indicate drier conditions. This either implies that climate could have varied even during dominance of the SHW and/or that local effects could have caused local responses (Pendall et al., 2001). It is also likely that the responses of many climate proxies are not fully understood and that qualitative estimates vary, both between proxies and how they are interpreted.

The strength of the SHW is mainly determined by the temperature gradient in the southern ocean, and the core of the SHW denotes the area of the steepest gradient. The extent of sea-ice cover around Antarctica has also been shown to influence the position of the SHW. Records from the Antarctic Peninsula imply a complex mid-Holocene temperature pattern and associated changes in the westerlies (Bentley et al., 2009). The Palmer Deep west of the Antarctic Peninsula experienced warming (Domack, 2002), while the Atlantic sector at the same time experienced cooling and expansion of sea-ice (Nielsen et al., 2004) in the mid-Holocene. In the Pacific the SHW and the Antarctic Circum Polar Current (ACC) generally display the same path and reconstructions from marine sediment cores show a southward shift of the ACC between 7800 and 5500 cal BP (Lamy et al., 2002). A southward displacement of the SHW and the ACC, synchronous with an expansion of sea-ice in the South Atlantic, would cause a very steep temperature gradient, which could explain the strengthening of the SHW inferred from our data. How far south the centre of the SHW extended is difficult to say due to the complex situation along the Antarctic Peninsula (Bentley et al., 2009), but it is evident from our data that it reached as far south as 54°S.

After 4500 cal BP Br, K, Ti, Zr, and Sr decline, and magnetic susceptibility is low. In combination with the large changes in diatom assemblages (mainly Zone III), we can infer lower precipitation, weaker winds and possibly cooler conditions. This is probably an effect of weaker SHW and/or of its displacement. Further north at Lago Cardiel (49°S), Gilli et al. (2005) have documented increasing wind speeds during the mid-Holocene. A gradual northward displacement of the SHW is further suggested by increased precipitation after 4000 cal BP at 41°S in Chile (Lamy et al., 2001), perhaps as a consequence of increased seasonality during the middle to late Holocene (Markgraf et al., 1992). Such a change in seasonality could explain the higher Mn/Fe ratios in our data set after 4500 cal BP; these indicate more oxic lake-water conditions and more vigorous spring and autumn overturns in the lake as a result of higher seasonality. This could have been one process to improve the oxic state of the bottom waters.

Tonello et al. (2009) have recently attempted to quantify Holocene precipitation in Patagonia by calibrating recent vegetation and precipitation (between 52 and 46°S, and between 73 and 68°W) to the pollen analysis from Cerro Frias site at c. 50°S and 73°W. Their transfer functions show significantly increased precipitation (c. 30%) between 12000 and 7000 cal BP, followed by a fairly constant precipitation between 7000 and 3500 cal BP and with a distinct decline after 3500 cal BP. However, Isla de los Estados' peripheral location more than 400 km southeast of Cerro Frias, makes a direct comparison difficult, not only to this site, but also to many of the other cited study sites.

Although the above described patterns in general concur with lower precipitation and windiness after 4500 cal BP in our data, this does not concur with the interpretations of bog hydrology and fire records from southern Patagonia (Huber et al., 2004). In Antarctica, the data of Björck et al. (1996) from east of the Antarctic Peninsula show a climatic optimum, warmer and more humid, between 4500 and 3300 cal BP and Bentley et al. (2009) infer a more southerly position of the SHW as one possible explanation of a prominent warming after 4500 cal BP. These apparently conflicting results, with either a northwards or southwards moving zone of the SHW, indicate that the pattern of temperatures and rainfall and their relationship are complex. It may not only involve latitudinal shifts of the SHW and sea-ice, but could also comprise other parts of the large-scale weather pattern such as the Southern Ocean circulation as well as features such as strengthening or weakening, broadening or focusing of the atmospheric circulation system. This can result in blocking off different air-masses, which eventually affect various regions differently.

At around 2500 cal BP K, Sr and Zr increase together with a small increase in magnetic susceptibility (Figs. 8 and 9), while the diatom assemblage (Zone IIIb) implies that the lake began to grow over. This coincides with reported glacier advances in Patagonia (Glasser et al., 2004) and with the end of the Holocene optimum on the Antarctic Peninsula (Bentley et al., 2009). The change post-dates reported changes in peat bogs and lakes on Tierra del Fuego and in southern Patagonia, which have been suggested to be part of a global event caused by weaker solar forcing around 2800–2700 cal BP (van Geel et al., 2000; Chambers et al., 2007). However, we see no such event in our records and the change at 2500 cal BP in the CAS sequence takes place not long time before the transition from lacustrine sediments to peat. It is therefore difficult to establish this as part of a true signal of changing climate.

No evidence for changes related to either the Medieval Warm Period or the Little Ice Age can be seen in our records, as the youngest part of the CAS sequence (and also the LGB record) consists of peat. This limits the use of XRF and our possibilities for climate inferences. However, the two records show some distinct susceptibility peaks during the last c. 800 years, which could imply periods of windier climate with increased beach erosion.

5.2. Holocene sea-level changes at Isla de los Estados

As indicated above, the proximity to the sea and with a position inside a raised beach make LGB a good sensor of relative sea-level changes. Having been glaciated during the Last Glacial Maximum and being part of the tectonically active Fuegian Andes, Isla de los Estados may have experienced a complex isostatic/tectonic history during the Holocene. For example, tectonic uplift has been suggested to explain young raised beach ridges in the Beagle Channel (Rabassa et al., 2000). It is, however, too far (700 km) from model predicted sites (Rostami et al., 2000), to invoke the same large-scale tectonics, connected with the subduction zone in the west, as in Patagonia.

Since Isla de los Estados was not heavily glaciated during the last glaciation (Rabassa et al., 2000; Möller et al., 2010), it is expected that local isostatic rebound was fairly restricted. Therefore the dominating relative sea-level change should be coupled to the global eustatic sea-level rise after the last deglaciation of the continental ice sheets, and possibly with a secondary (and later) influence from isostatic and tectonic movements.

The large and shallow shelf north of Isla de los Estados (Fig. 1) was most likely dry land during LGM. The shelf area immediately north of Bahia Colnett is very shallow: the −20 m contour line is situated c. 2 km north of the shore and water depths of only 50 m are found at least 8–10 km further out. With the combination of a restricted ice load and early deglaciation (Unkel et al., 2008; Möller et al., 2010) it is not surprising that the first indications of a marine influence in LGB appear as late as a few millennia into the Holocene (Fig. 6).

From interpretations of the LGB stratigraphy and proxies, we have estimated that the area experienced a sea-level rise of 2–4 m between 8500 and 6500 cal BP (Fig. 6). This order of magnitude is compatible with the estimated global sea-level rise at that time (Fleming et al., 1998; Lambeck and Chappell, 2001). Within this period, around 7600 cal BP, Yu et al. (2007) have indications of rapidly rising sea level (1 cm/yr), which they relate to abrupt decay of the Labrador ice sheet. It is therefore very likely that our rising sea level at that time was dominated by the global eustatic signal. The end of the transgression roughly coincides with the final melting of the large continental ice sheets and when global sea level had approximately already reached today's level (Bird et al., 2007). The subsequent almost 3000 years of more or less stable sea level (Fig. 6), implies a fairly long mid-Holocene high-stand, also shown in many far field locations (Woodroffe and Horton, 2005). In this context it is noteworthy that the highest mid-Holocene littoral deposits along the Beagle Channel, 200–300 km west of Isla de los Estados and dated to 6500–5500 cal BP, occur at 3–5 m a.s.l. in the eastern part and at 8–10 m a.s.l. in the western part of the Channel (Gordillo et al., 1992; Rabassa et al., 2000). This implies a westwards increasing glacial unloading effect since the mid-Holocene along the southernmost part of Tierra del Fuego, indicating that the last ice sheet was thicker in the inner part of the Beagle Channel. The stable sea level on Isla de los Estados therefore shows that any remaining isostatic effect had ceased here.

Our data further suggest that during the last 3500–4000 years relative sea level first dropped to at least between 1 and 2 m below present day sea level and then began to rise to present day levels (Fig. 6). As been pointed out by Rabassa and Clapperton (1990) and Bentley and McCulloch (2005) the region has been subject to complex neotectonic movements and we think that this may be one possible explanation for the regression after around 4000 cal BP. Another reason could be that Isla de los Estados is situated within Clark et al.'s (1978) region V where a late Holocene regression is a geodynamically expected feature, like in S Africa and Australia (Woodroffe and Horton, 2005). In the Pacific region it has also been suggested that migration of the geoid (Grossman et al., 1998) or climate change (Moriwaki et al., 2006), such as increased El Niño, could explain a late Holocene low stand. Changes in the local or regional wind conditions could also be an explanatory factor. Less vigorous storms and windy conditions, such as we have inferred from our Lake Cascada record after 4500 cal BP, should have decreased the vulnerability of any protecting beach ridge. Under such conditions the inferred so-called boundary conditions for maintaining a fresh-water basin (2 m above mean sea level) would have been less.

How low the supposed regression reached is impossible to estimate from our data, but it may only have reached c. 2 m below today's sea level. Today the local sea level is rising, which is evident from the erosion of beach ridges on Isla de los Estados as well as the erosion of the beach and former harbor area of the more than a century old prison in Puerto Cook (Fig. 1). However, it is not possible to specify when this rise began.

Increased mean maximum wave height, as an effect of the increased storminess since 800 cal BP that we have inferred from our Cascada record, and the dynamics of the beach ridges enclosing the basin may have contributed to the transgression we see both in the youngest stratigraphic record and as a changing coast. Nevertheless, the global ongoing sea-level rise could also have played a noteworthy role for the apparent transgression, and the area may therefore also be a good example on how small sea-level changes can alter the equilibrium of dynamic coastal systems and their processes.

6. Conclusions

The peat and gyttja core of Lago Galvarne Bog and the lake sediment core of Laguna Cascada, both dating back slightly more than 16 ka cal BP (Unkel et al., 2008), reveal an unprecedented record of the Holocene and the end of the last glacial on Isla de los Estados in southernmost Patagonia.

Both cores provide a continuous record from the early Holocene until c. 1000 cal BP, as our age–depth models show (Figs. 3 and 7), based on lithological boundaries and dense AMS-^{14}C dating (Table 1), in combination with the software OxCal 4.0 (Bronk Ramsey, 2008).

Geochemical analyses through high resolution XRF scanning for the sediment sequences and through TC, TN and LOI analyses of the lake sediments and the peat sequences provide information on hydrologic changes at both sites and also give a general idea of the environmental and climatic development of the study area. Diatom analyses support the geochemical records from Laguna Cascada, showing distinct changes in water level and mixing, alkalinity and trophic status of the lake (Fig. 8).

We interpret the results from both sites as being influenced by two different forcings through much of the Holocene: while the coastal site of Lago Galvarne Bog, behind a dynamic beach ridge, was very susceptible to effects of local relative sea-level changes, Laguna Cascada recorded mainly changes in the regional climate setting, largely affected by the varying strength and position of the Southern Hemisphere Westerlies (SHW).

With respect to the variations of the SHW and in good agreement with other records from Patagonia and adjacent regions (Lamy et al., 2001, 2002; Glasser et al., 2004; Gilli et al., 2005; Bentley et al., 2009) our combined proxy records show increased windiness, increased precipitation and higher surface run-off between 8500 and 4500 cal BP. This was possibly due to a more poleward position or a general strengthening/focusing of the SHW. After 4500 cal BP, several geochemical proxies, magnetic susceptibility and the changes in diatom assemblages from Laguna Cascada indicate lower precipitation, decreased wind speed and slightly cooler conditions. This was probably due to a gradual northward displacement of the SHW. Increased seasonality during the middle to late Holocene as reported by Markgraf et al. (1992) could explain the higher Mn/Fe ratios in our data after 4500 cal BP indicating more oxic lake-water conditions. Around 1000 cal BP the sedimentation at the marginal coring site of Laguna Cascada changed from gyttja to peat, partly due to a lake level lowering.

According to the diatom data this process started already around 2500 cal BP, which coincides with reported glacier advances in Patagonia (Glasser et al., 2004) and with the end of the Holocene optimum on the Antarctic Peninsula (Bentley et al., 2009). The cooler and wetter climate of middle and late Holocene may have intensified organic matter accumulation in littoral zones of lakes, influencing lake-water chemistry and habitat availability. Such ecological or biogeochemical changes in the watershed may also exert important controls on the diatom assemblages recorded in lake sediment cores (Anderson, 2000). In the most recent decades, increased diatom production may reflect not just warmer temperatures, but nutrient enrichment from, for example, atmospheric deposition (Wolfe et al., 2006). However, also local conditions, such as the character of shoreline vegetation need to be taken into consideration to explain complex relationships between climate and diatom communities (Finkelstein and Gajewski, 2007).

Based on our interpretations of the Lago Galvarne Bog stratigraphy and proxies, we conclude that the area experienced a sea-level rise of 2–4 m between 8500 and 6500 cal BP (Fig. 6), which is in the same order of magnitude as the estimated global sea-level rise at that time (Fleming et al., 1998; Lambeck and Chappell, 2001). The onset of gyttja sedimentation around 7900 cal BP shows that the former peat site had turned into an aquatic sedimentation basin. The chemical data at Lago Galvarne Bog indicate gradually increasing marine influence, probably as a combined effect of rising sea level and thereby increased impact of storms and maximum high tides. This rise in sea level must have been dominated by the global eustatic signal, and the following stable sea level shows that any previous isostatic effect had

terminated since global sea level had already reached approximately today's level (Bird et al., 2007). After this marine high-stand in the mid-Holocene, the Lago Galvarne Bog turned into a peat bog around 3400 cal BP. This change from a stable to a regressive sea-level development can be explained by several different factors: neotectonics, climate, migration of the geoid or by general global mass displacement. Today the local sea level is rising, which is evident from the erosion of beach ridges on Isla de los Estados.

Acknowledgements

The position of Ingmar Unkel was funded by the German Research Council (DFG scholarship No. Un261/2-1). The research expedition to Isla de los Estados was carried out by Charlie Porter's ketch "Ocean Tramp" (Puerto Williams) and funded by a grant (621-2003-3611) to SB from the Swedish Research Council (VR) as part of his so-called Atlantis project. The field work at the two sites was carried out by SB, BW, KL and J. F. Ponce (Ushuaia). The analytical and logistic costs were funded both by the VR grant, by Kungliga Fysiografiska Sällskapet in Lund and the Swedish Polar Secretariat. Two anonymous reviewers gave valuable comments to improve our manuscript. To these persons and institutions we would like to express our sincere thanks.

Appendix A. Supplementary data

Supplementary data to this article can be found online at doi:10.1016/j.gloplacha.2010.07.003.

References

Abella, S.E.B., 1988. The effect of the Mt. Mazama ashfall on the planktonic diatom community of lake Washington. Limnology and Oceanography 33, 1376–1385.
Anderson, N.J., 2000. Diatoms, temperature and climatic change. European Journal of Phycology 35 (04), 307–314.
Bentley, M.J., McCulloch, R.D., 2005. Impact of neotectonics on the record of glacier and sea level fluctuations, Strait of Magellan, Southern Chile. Geografiska Annaler: Series A, Physical Geography 87, 393–402. doi:10.1111/j.0435-3676.2005.00265.x.
Bentley, M.J., Hodgson, D.A., Smith, J.A., Cofaigh, C.O., Domack, E.W., Larter, R.D., Roberts, S.J., Brachfeld, S., Leventer, A., Hjort, C., Hillenbrand, C.D., Evans, J., 2009. Mechanisms of Holocene palaeoenvironmental change in the Antarctic Peninsula region. Holocene 19, 51–69. doi:10.1177/0959683608096603.
Bird, M.I., Fifield, L.K., Teh, T.S., Chang, C.H., Shirlaw, N., Lambeck, K., 2007. An inflection in the rate of early mid-Holocene eustatic sea-level rise: a new sea-level curve from Singapore. Estuarine, Coastal and Shelf Science 71, 523–536. doi:10.1016/j.ecss.2006.07.004.
Birks, H.J.B., Lotter, A.F., 1994. The impact of the Laacher See Volcano (11 000 yr B.P.) on terrestrial vegetation and diatoms. Journal of Paleolimnology 11, 313–322. doi:10.1007/BF00677991.
Björck, S., Olsson, S., Ellis-Evans, C., Håkansson, H., Humlum, O., de Lirio, J.M., 1996. Late Holocene palaeoclimatic records from lake sediments on James Ross Island, Antarctica. Palaeogeography, Palaeoclimatology, Palaeoecology 121, 195–220. doi:10.1016/0031-0182(95)00086-0.
Björck, S., Hjort, C., Ljung, K., Möller, P., Wohlfarth, B., 2007. Isla de los Estados—Quaternary geology and palaeoclimatology at the end of the world. In: Rickberg, S. (Ed.), Polarforskningssekretariatets Årsbok 2006. Stockholm, pp. 44–49.
Bronk Ramsey, C., 2001. Development of the radicocarbon calibration program. Radiocarbon 43, 355–363.
Bronk Ramsey, C., 2008. Deposition models for chronological records. Quaternary Science Reviews 27, 42–60. doi:10.1016/j.quascirev.2007.01.019.
Caminos, R., Nullo, F., 1979. Descriptión Geológica de la Hoja 67 e, Isla de los Estados. Servicio Geológico Nacional, Buenos Aires.
Chambers, F.M., Mauquoy, D., Brain, S.A., Blaauw, M., Daniell, J.R.G., 2007. Globally synchronous climate change 2800 years ago: proxy data from peat in South America. Earth and Planetary Science Letters 253, 439–444. doi:10.1016/j.epsl.2006.11.007.
Clark, J.A., Farrell, W.E., Peltier, W.R., 1978. Global changes in postglacial sea level: a numerical calculation. Quaternary Research 9 (3), 265–287. doi:10.1016/0033-5894(78)90033-9.
Cleve-Euler, A. (1951–1955). Die Diatomeen von Schweden und Finnland. *Kungliga Vetenskapsakademiens Handlingar* 2–5, 2: (1951) 1–163; 3:3 (1952) 1–153; 4:1 (1953) 1–255; 4:5 (1953) 1–158; 5:4 (1955) 1–232.
Croudace, I.W., Rindby, A., Rothwell, R.G., 2006. ITRAX: description and evaluation of a new multi-function X-ray core scanner. Geological Society Special Publication 267, 51–63.
Dalziel, I.W.D., Caminos, R., Palmer, K.F., Nullo, F., Casanova, R., 1974. South extremity of Andes: Geology of Isla de los Estados, Argentine Tierra del Fuego. American Association of Petroleum Geologists Bulletin 58, 2502–2512.
Davison, W., 1993. Iron and manganese in lakes. Earth Science Reviews 34, 119–163.
Dillon, P.J., Molot, L.A., 1997. Effect of landscape form on export of dissolved organic carbon, iron, and phosphorus from forested stream catchments. Water Resources Research 33, 2591–2600. doi:10.1029/97WR01921.
Domack, E.W., 2002. A synthesis for Site 1098: Palmer Deep. In: Barker, P.F., Camerlenghi, A., Acton, G.D., Ramsay, A.T.S. (Eds.), Proceedings of the Ocean Drilling Program, Scientific Results, Volume 178, pp. 1–14. [online].
Dudley, T.R., Crow, G.E., 1983. A contribution to the flora and vegetation of Isla de los Estados (Staten Island), Tierra del Fuego, Argentina. Antarctic Research Series, Terrestrial Biology II 37 27 pp.
Engstrom, D.R., Wright, H.E.J., 1984. Chemical stratigraphy of lake sediments as a record of environmental change. In: Haworth, E.Y., Lund, J.W.G. (Eds.), Lake Sediments and Environmental History. Leicester University Press, pp. 11–68.
Finkelstein, S.A., Gajewski, K., 2007. A palaeolimnological record of diatom-community dynamics and late-Holocene climatic changes from Prescott Island, Nunavut, central Canadian Arctic. Holocene 17 (6), 803–812. doi:10.1177/0959683607080521.
Fleming, K., Johnston, P., Zwartz, D., Yokoyama, Y., Lambeck, K., Chappell, J., 1998. Refining the eustatic sea-level curve since the Last Glacial Maximum using far- and intermediate-field sites. Earth and Planetary Science Letters 163, 327–342. doi:10.1016/S0012-821X(98)00198-8.
Flower, R., 2005. A taxonomic and ecological study of diatoms from freshwater habitats in the Falkland Islands. Diatom Research 20, 23–96.
Gilli, A., Ariztegui, D., Anselmetti, F.S., McKenzie, J.A., Markgraf, V., Hajdas, I., McCulloch, R.D., 2005. Mid-Holocene strengthening of the Southern Westerlies in South America—sedimentological evidences from Lago Cardiel, Argentina (49°S). Global and Planetary Change 49, 75–93.
Glasser, N., Harrison, S., Winchester, V., Aniya, M., 2004. Late Pleistocene and Holocene palaeoclimate and glacier fluctuations in Patagonia. Global and Planetary Change 43, 79–101.
Gordillo, S., Bujalesky, G.G., Pirazzoli, P.A., Rabassa, J.O., Saliège, J.-F., 1992. Holocene raised beaches along the northern coast of the Beagle Channel, Tierra del Fuego, Argentina. Palaeogeography, Palaeoclimatology, Palaeoecology 99, 41–54. doi:10.1016/0031-0182(92)90006-Q.
Grimm, E.C., 1991. TILIA and TILIAGRAPH Software. Illinois State Museum. Research & Collection Center, Springfield, Illinois.
Grossman, E.E., Fletcher III, C.H., Richmond, B.M., 1998. The Holocene sea-level highstand in the equatorial Pacific: analysis of the insular paleosea-level database. Coral Reefs 17 (3), 309–327. doi:10.1007/s003380050132.
Harper, M.A., Howorth, R., McLeod, M., 1986. Late Holocene diatoms in Lake Poukawa: effects of airfall tephra and changes in depth. New Zealand Journal of Marine and Freshwater 20, 107–118.
Huber, U.M., Markgraf, V., Schäbitz, F., 2004. Geographical and temporal trends in Late Quaternary fire histories of Fuego-Patagonia, South America. Quaternary Science Reviews 23, 1079–1097.
Hustedt, F., 1930-1966. Die Kieselalgen Deutschlands, Österreichs und der Schweiz - unter Berücksichtigung der übrigen Länder Europas sowie der angrenzenden Meersgebiete. Rabenhorst's Kryptogamen-Flora VII. Akademischer Verlag, Leipzig, p. 2581.
Kilian, R., Hohner, M., Biester, H., Wallrabe-Adams, H.J., Stern, C.R., 2003. Holocene peat and lake sediment tephra record from the southernmost Chilean Andes (53–55°S). Revista Geologica de Chile 30, 47–64.
Kilroy, C., Sabbe, K., Bergey, E.A., Vyverman, W., Lowe, R., 2003. New species of *Fragilariforma* (Bacillariophyceae) from New Zealand and Australia. New Zealand Journal of Botany 41, 535–554.
Koinig, K.A., Shotyk, W., Lotter, A.F., Ohlendorf, C., Sturm, M., 2003. 9000 years of geochemical evolution of lithogenic major and trace elements in the sediment of an alpine lake—the role of climate, vegetation and landuse history. Journal of Paleolimnology 30, 307–320. doi:10.1023/A:1026080712312.
Köster, D., Pienitz, R., 2006. Late-Holocene environmental history of two New England ponds: natural dynamics versus human impacts. Holocene 16, 519–532. doi:10.1191/0959683606hl947rp.
Krammer, K., Lange-Bertalot, H., 1986. Bacillariophyceae 1. Teil: Naviculaceae. In: Ettl, H., Gerloff, J., Heynig, H., Mollenhauer, D. (Eds.), Süßwasserflora von Mitteleuropa 2 (1). Gustav Fischer Verlag, Stuttgart, New York, p. 876.
Krammer, K., Lange-Bertalot, H., 1988. Bacillariophyceae 2. Teil: Bacillariaceae, Epithemiaceae, Surirellaceae. In: Ettl, H., Gerloff, J., Heynig, H., Mollenhauer, D. (Eds.), Süsswasserflora von Mitteleuropa 2(2). Gustav Fischer Verlag, Stuttgart, New York, p. 596.
Krammer, K., Lange-Bertalot, H., 1991a. Bacillariophyceae 3. Teil: Centrales, Fragilariaceae, Eunotiaceae. In: Ettl, H., Gerloff, J., Heynig, H., Mollenhauer, D. (Eds.), Süsswasserflora von Mitteleuropa 2(3). Gustav Fischer Verlag, Stuttgart, New York, p. 576.
Krammer, K., Lange-Bertalot, H., 1991b. Bacillariophyceae 4. Teil: Achnanthaceae. Kritische Ergänzungen zu Navicula (Lineolatae) und Gomphonema. In: Ettl, H., Gärtner, J., Gerloff, J., Heynig, H., Mollenhauer, D. (Eds.), Süsswasserflora von Mitteleuropa 2(4). Gustav Fischer Verlag, Stuttgart, New York, p. 437.
Lambeck, K., Chappell, J., 2001. Sea level change through the last glacial cycle. Science 292, 679–686. doi:10.1126/science.1059549.
Lamy, F., Hebbeln, D., Röhl, U., Wefer, G., 2001. Holocene rainfall variability in southern Chile: a marine record of latitudinal shifts of the Southern Westerlies. Earth and Planetary Science Letters 185, 369–382.
Lamy, F., Rühlemann, C., Hebbeln, D., Wefer, G., 2002. High- and low-latitude climate control on the position of the southern Peru–Chile Current during the Holocene. Paleoceanography 17. doi:10.1029/2001PA000727.
Lotter, A.F., Birks, H.J.B., Zolitschka, B., 1995. Late-glacial pollen and diatom changes in response to two different environmental perturbations: volcanic eruption and

Younger Dryas cooling. Journal of Paleolimnology 14, 23–47. doi:10.1007/BF00682592.
Markgraf, V., Dodson, J.R., Kershaw, A.P., McGlone, M.S., Nicholls, N., 1992. Evolution of Late Pleistocene and Holocene climates in the circum-South Pacific land areas. Climate Dynamics 6, 193–211.
Mayewski, P.A., Rohling, E.E., Curt Stager, J., Karlén, W., Maasch, K.A., David Meeker, L., Meyerson, E.A., Gasse, F., van Kreveld, S., Holmgren, K., Lee-Thorp, J., Rosqvist, G., Rack, F., Staubwasser, M., Schneider, R.R., Steig, E.J., 2004. Holocene climate variability. Quaternary Research 62, 243–255. doi:10.1016/j.yqres.2004.07.001.
McCormac, G., Hogg, A.G., Blackwell, P.G., Buck, C.E., Higham, T.F.G., Reimer, P.J., 2004. SHCal04 southern hemisphere calibration, 0–11.0 cal kyr BP. Radiocarbon 46, 1087–1092.
Meyers, P.A., Teranes, J.L., 2001. Sediment organic matter. In: Last, W.M., Smol, J.P. (Eds.), Tracking Environmental Change Using Lake Sediments. Kluwer Academic Publishers, Dordrecht, pp. 239–269.
Möller, P., Hjort, C., Björck, S., Rabassa, J., Ponce, J.F., 2010. Late Quaternary glaciation history of Isla de los Estados, southeasternmost South America. Quaternary Research 73 (3), 521–534. doi:10.1016/j.yqres.2010.02.004.
Moriwaki, H., Chikamori, M., Okuno, M., Nakamura, T., 2006. Holocene changes in sea level and coastal environments on Rarotonga, Cook Islands, South Pacific Ocean. Holocene 16 (6), 839–848. doi:10.1191/0959683606hol976rp.
Nagumo, T., Kobayashi, H., 1977. Proposal of *Melosira arentii* (Kolbe) comb. nov. based on light and electron microscopy. Bulletin of the Japanese Society of Phycology 25, 182–1988.
Nielsen, S.H.H., Koç, N., Crosta, X., 2004. Holocene climate in the Atlantic sector of the Southern Ocean: controlled by insolation or oceanic circulation? Geology 32, 317–320. doi:10.1130/G20334.1.
Pace, M.L., Cole, J.J., 2002. Synchronous variation of dissolved organic carbon and color in lakes. Limnology and Oceanography 47, 333–342.
Patrick, R., and Reimer, C. W. (1966–1977). The diatoms of the United States (excl. of Alaska and Hawaii). The Academy of Natural Sciences of Philadelphia Vol. 1&2, Monograph 13, 688 pp.
Pendall, E., Markgraf, V., White, J.W.C., Dreier, M., Kenny, R., 2001. Multiproxy record of late Pleistocene–Holocene climate and vegetation changes from a peat bog in Patagonia. Quaternary Research 55, 168–178.
Pienitz, R., Vincent, W.F., 2000. Effect of climate change relative to ozone depletion on UV exposure in subarctic lakes. Nature 404, 484–487. doi:10.1038/35006616.
Rabassa, J., Clapperton, C.M., 1990. Quaternary glaciations of the southern Andes. Quaternary Science Reviews 9, 153–174. doi:10.1016/0277-3791(90)90016-4.
Rabassa, J., Coronato, A., Bujalesky, G., Salemme, M., Roig, C., Meglioli, A., Heusser, C., Gordillo, S., Roig, F., Borromei, A., Quattrocchio, M., 2000. Quaternary of Tierra del Fuego, Southernmost South America: an updated review. Quaternary International 68–71, 217–240.
Risacher, F., Fritz, B., 2000. Bromine geochemistry of salar de Uyuni and deeper salt crusts, Central Altiplano, Bolivia. Chemical Geology 167, 373–392. doi:10.1016/S0009-2541(99)00251-X.
Rostami, K., Peltier, W.R., Mangini, A., 2000. Quaternary marine terraces, sea-level changes and uplift history of Patagonia, Argentina: comparisons with predictions of the ICE-4G (VM2) model of the global process of glacial isostatic adjustment. Quaternary Science Reviews 19 (14–15), 1495–1525. doi:10.1016/S0277-3791(00)00075-5.
Round, F.E., Crawford, R.M., Mann, D.G., 1990. The Diatoms. Biology and Morphology of the Genera. Cambridge University Press, Cambridge.
Rumrich, U., Lange-Bertalot, H., Rumrich, M., 2000. Diatoms of the Andes. Annotated diatom monographs. In: Lange-Bertalot, H. (Ed.), Iconographia Diatomologica, Vol. 9. Koeltz Scientific Books, Königstein, p. 671.
Sholkovitz, E.R., 1978. The flocculation of dissolved Fe, Mn, Al, Cu, Ni, Co and Cd during estuarine mixing. Earth and Planetary Science Letters 41, 77–86. doi:10.1016/0012-821X(78)90043-2.
Snyder, M., Taillefert, M., Ruppel, C., 2004. Redox zonation at the saline-influenced boundaries of a permeable surficial aquifer: effects of physical forcing on the biogeochemical cycling of iron and manganese. Journal of Hydrology 296, 164–178. doi:10.1016/j.jhydrol.2004.03.019.
Song, Y., Müller, G., 1993. Freshwater sediments: sinks and sources of Bromine. Die Naturwissenschaften 80, 558–560. doi:10.1007/BF01149270.
Sparrenbom, C.J., Bennike, O., Björck, S., Lambeck, K., 2006. Holocene relative sea-level changes in the Qaqortoq area, southern Greenland. Boreas 35, 171–187. doi:10.1080/03009480600578032.
Sterken, M., Verleyen, E., Sabbe, K., Terryn, G., Charlet, F., Bertrand, S., Boës, X., Fagel, N., De Batist, M., Vyverman, W., 2008. Late Quaternary climatic changes in southern Chile, as recorded in a diatom sequence of Lago Puyehue (40°40′S). Journal of Paleolimnology 39, 219–235. doi:10.1007/s10933-007-9114-1.
Stern, C., 2008. Holocene tephrochronology record of large explosive eruptions in the southernmost Patagonian Andes. Bulletin of Volcanology 70, 435–454. doi:10.1007/s00445-007-0148-z.
Taubenheim, J., 1969. Statistische Auswertung geophysikalischer und meteorologischer Daten. Akademische Verlagsgesellschaft Geest u, Portig, Leipzig.
Telford, R.J., Barker, P., Metcalfe, S., Newton, A., 2004. Lacustrine responses to tephra deposition: examples from Mexico. Quaternary Science Reviews 23, 2337–2353. doi:10.1016/j.quascirev.2004.03.014.
Tonello, M.S., Mancini, M.V., Seppä, H., 2009. Quantitative reconstruction of Holocene precipitation changes in southern Patagonia. Quaternary Research 72, 410–420. doi:10.1016/j.yqres.2009.06.011.
Trauth, M.H., 2006. MATLAB Recipes for Earth Sciences. Springer, Berlin Heidelberg New York.
Ullman, W.J., 1995. The fate and accumulation of bromide during playa salt deposition: an example from Lake Frome, South Australia. Geochimica et Cosmochimica Acta 59, 2175–2186. doi:10.1016/0016-7037(95)00099-L.
Unkel, I., Björck, S., Wohlfarth, B., 2008. Deglacial environmental changes on Isla de los Estados (54.41S), southeastern Tierra del Fuego. Quaternary Science Reviews 27, 1541–1554. doi:10.1016/j.quascirev.2008.05.004.
Van Dam, H., Mertens, A., Sinkeldam, J., 1994. A coded checklist and ecological indicator values of freshwater diatoms from The Netherlands. Aquatic Ecology 28 (1), 117–133. doi:10.1007/BF02334251.
van Geel, B., Heusser, C.J., Renssen, H., Schuurmans, C.J.E., 2000. Climatic change in Chile at around 2700 BP and global evidence for solar forcing: a hypothesis. Holocene 10, 659–664. doi:10.1191/09596830094908.
Wolfe, A., Cooke, C., Hobbs, W., 2006. Are current rates of atmospheric nitrogen deposition influencing lakes in the eastern Canadian Arctic? Arctic, Antarctic, and Alpine Research 38 (3), 465–476. doi:10.1657/1523-0430(2006) 38 465:ACROAN 2.0.CO;2.
Woodroffe, S.A., Horton, B.P., 2005. Holocene sea-level changes in the Indo-Pacific. Journal of Asian Earth Sciences 25 (1), 29–43. doi:10.1016/j.jseaes.2004.01.009.
Yu, S.-Y., Berglund, B.E., Sandgren, P., Lambeck, K., 2007. Evidence for a rapid sea-level rise 7600 yr ago. Geology 35, 891–894. doi:10.1130/g23859a.1.